

Gluon density and F_2 functions from BK equation with local impact parameter dependence in DIS on nuclei

S. Bondarenko ^{a,b)} *

^{a)} *Leaving University Santiago De Compostela, Spain.*

^{b)} *Ariel University, Israel.*

November 30, 2018

Abstract

The DIS process on nuclei is considered in the framework of LO BK equation with local impact parameter dependence. The initial conditions of GBW type, found in [4], was used in the solution of BK equation. Integrated gluon density function and F_2 nucleus structure function for different nuclei are calculated. Obtained results are compared with the different parameterizations of integrated gluon density function from [5, 6, 7, 8]. The anomalous dimensions and saturation scales for different nuclei are calculated at different energies. The expressions of the functional form of saturation scale are obtained for the proton and different nuclei as functions of the impact parameter and energy.

1 Introduction

The phenomenological applications of the QCD BFKL Pomeron, [1], and of the system of interacting Pomerons, [9, 10], could be investigated in the framework of the BK equation [2, 3]. This framework was used in the calculations of the amplitudes of the different scattering processes, see [11, 12, 13, 14, 15, 16] for example and references therein. The same principals of the saturation physics were applied in the different phenomenological and CGC type models as well, see [17, 18, 19, 20, 21, 22, 25, 24, 26, 29, 30, 31, 32]. In these approaches, inspired by BK equation, the impact parameter dependence of the solution of the equation was treated only approximately, see for example [23, 25], whereas the phenomenological models, such as GBW model [17, 18], treating the impact parameter dependence neglect the evolution of the amplitude with rapidity. There are also the studies of the impact parameter dependence of gluon structure function together with DGLAP evolution of the function considered in the papers [28, 19, 29, 32] and calculations of the unintegrated gluon density

*Email: sergeyb@ariel.ac.il

function in the framework of modified BK equation with the factorized dependence of impact parameter and momentum in initial conditions in [33, 34, 35]. Nevertheless, the investigation of the BK equation with the new type of the initial conditions with the non-factorized impact parameter and momentum dependence is a task which requires a deep attention due the importance of the BK equation in the different scattering processes with nuclei involved.

In the paper [4] a first step towards the including of the impact parameter dependence into the rapidity evolution of the scattering amplitude through initial conditions was made. It must be stressed, that introducing local impact parameter dependence into evolution equation through initial condition we miss the precise treatment of transverse position in the evolution kernel, that does not allow to calculate the contribution of the Pomeron loops into the amplitude, for example. Nevertheless, considered semi-classical framework with local impact parameter dependence is justified due the following observation. For the scattering on the target, which size is large, the momentum transfer of the Pomeron line originating from the external particle is bounded by the form-factors of the sources, and, therefore, it is small for the nuclei (and possibly proton) targets. Therefore, when we consider only "net" diagram structure, i.e. the semi-classical approximation to the problem, and when we do not account the Pomeron loops contribution, the constraint on the momentum transfer of the Pomeron line is imposed on the all Pomeron lines that justify our approximation, see more details in [12] and references therein.

The DIS process on the proton, which was considered in the paper [4], allowed to find a initial condition for the BK evolution by the fitting of the F_2 function data. In the present studies we use the same as in [4] calculation procedure solving LO BK equation in each point of the impact parameter space, using methods developed in [12]. The difference with the calculations from [4] is that now we consider different nuclei as a target instead the proton target in the paper [4], and, therefore, the impact parameter profile of the proton we change on the Wood-Saxon parameterization of the nuclei density profile. All other parameters of the initial profile for BK equation we take the same, in spite of the differences of the processes. The applicability of this assumption we will discuss latter. As it will be shown, the change of only impact parameter profile in initial conditions will lead to the results for integrated gluon density function similar to the results of the different calculations of the same function in [5, 6, 7, 8], justifying this minimal modifications of the initial conditions for DIS on nuclei.

The comparison of our results with the results of other calculations is based on the fact, that due the lack of the high energy DIS process data for the nuclei targets, we could not perform the fitting of the data in order to determine all parameters for initial conditions as it was done in [4]. More of that, we also could not use the low energy data for this purpose, because the small Bjorken x evolution begins at the energies larger than the energies for which the nuclei data are known. Fortunately, the existing models of the integrated gluon density, [5, 6, 7, 8], allow to extrapolate the integrated gluon density function till very small values of x , $x \approx 10^{-7}$. It gives to us a possibility to check how good (or bad) our calculations are and, therefore, how good (or bad) our initial conditions are. To our surprise, curves for the integrated gluon density of different nuclei obtaining in our framework are in the "window" of the curves from the [5, 6, 7, 8] which were calculated in different approaches. This result, as we underlined previously, justify the use of "minimal changed" initial conditions for the nuclei in our calculations.

The knowledge of the unintegrated gluon density function, i.e. solution of BK equation, allows to find other functions and parameters connected with the DIS process. We calculate the integrated gluon density function and F_2 structure function of the DIS process on nuclei, or, more precisely the proton-nuclei ratio of these functions. In this case we find a parameterization of the nuclei integrated gluon density and F_2 functions

in the terms of the corresponding proton functions and number of nucleons in the nuclei. We also calculate a anomalous dimension of the integrated gluon density function, similarly to the calculations of [36], and find a saturation momenta of the process as a function of impact parameter space and energy.

This paper is organized as follows. In the next section we describe a formalism of the calculations. In Sec.3 we present obtained results for the integrated gluon density function. In Sec.4 we consider the calculations of the F_2 structure function and in Sec.5 we present results for the anomalous dimensions of the integrated gluon density function of the DIS process on the proton and on the nuclei. The saturation scale calculations for the problem of DIS process on the proton and DIS process on the nuclei are presented in the Section 6. Section 7 is a conclusion of the paper.

2 The low-x structure function in the momentum representation

In this section we shortly remind the main formulae used in the following calculations (see also [4]). The unintegrated gluon density function $f(x, k^2, b)$ of the DIS process we find solving BK equation for the each point in the impact parameter space:

$$\begin{aligned} \partial_y f(y, k^2, b) = & \frac{N_c \alpha_s}{\pi} k^2 \int \frac{da^2}{a^2} \left[\frac{f(a^2, b) - f(k^2, b)}{|a^2 - k^2|} + \frac{f(k^2, b)}{[4a^4 + k^4]^{\frac{1}{2}}} \right] \\ & - 2\pi \alpha_s^2 \left[k^2 \int_{k^2} \frac{da^2}{a^4} f(a^2, b) \int_{k^2} \frac{dc^2}{c^4} f(c^2, b) + f(k^2, b) \int_{k^2} \frac{da^2}{a^4} \log \left(\frac{a^2}{k^2} \right) f(a^2, b) \right] \end{aligned} \quad (1)$$

where we introduced the rapidity variable $y = \log(1/x)$. In Eq.1 we assumed, that the evolution is local in the transverse plane, i.e. impact parameter dependence of $f(y, k^2, b)$ appear only throw the initial condition for the $f(y, k^2, b)$ function

$$f(y = y_0, k^2, b) = f_{in}(k^2, b) \quad (2)$$

In order to exclude part of ambiguities in the solution of BK equation which arise due the absence of the NLO corrections, we perform the following substitute in the equation

$$f(y, k^2, b) \rightarrow \frac{f(y, k^2, b) \alpha_s(k^2)}{\alpha_s} = \frac{\tilde{f}(y, k^2, b)}{\alpha_s}, \quad (3)$$

obtaining

$$\begin{aligned} \partial_{\tilde{y}} \tilde{f}(\tilde{y}, k^2, b) = & \frac{N_c}{\pi} k^2 \int \frac{da^2}{a^2} \left[\frac{\tilde{f}(a^2, b) - \tilde{f}(k^2, b)}{|a^2 - k^2|} + \frac{\tilde{f}(k^2, b)}{[4a^4 + k^4]^{\frac{1}{2}}} \right] \\ & - 2\pi \left[k^2 \int_{k^2} \frac{da^2}{a^4} \tilde{f}(a^2, b) \int_{k^2} \frac{dc^2}{c^4} \tilde{f}(c^2, b) + \tilde{f}(k^2, b) \int_{k^2} \frac{da^2}{a^4} \log \left(\frac{a^2}{k^2} \right) \tilde{f}(a^2, b) \right] \end{aligned} \quad (4)$$

where $\tilde{y} = \alpha_s y$. The value of α_s is a constant in the LO approximation and we consider α_s as parameter of the model, which we borrow from the fit of DIS data performed in [4].

The impact factors, used latter in calculations of F_2 structure function, are usual impact factors of the problem with the three light quarks flavors of equal mass included. They have the following form (see [28] for example):

$$\Phi_L(k, m_q^2) = 32 \pi \alpha \sum_{q=1}^3 e_q^2 \int_0^1 d\rho d\eta \frac{k^2 \eta (1-\eta) \rho^2 (1-\rho)^2 Q^2}{(Q^2 \rho (1-\rho) + k^2 \eta (1-\eta) + m_q^2) (Q^2 \rho (1-\rho) + m_q^2)} \quad (5)$$

and

$$\Phi_T(k, m_q^2) = 4\pi\alpha \sum_{q=1}^3 e_q^2 \int_0^1 d\rho d\eta \cdot \frac{k^2 Q^2 (\rho^2 + (1-\rho)^2) \rho(1-\rho) (\eta^2 + (1-\eta)^2) + k^2 (\rho^2 + (1-\rho)^2) m_q^2 + 4\rho(1-\rho)\eta(1-\eta)m_q^2}{(Q^2\rho(1-\rho) + k^2\eta(1-\eta) + m_q^2) (Q^2\rho(1-\rho) + m_q^2)} \quad (6)$$

Due the including light quark masses in the calculations, the rapidity variable y (Bjorken x) in BK equation is also modified, see details in [17, 18]. For each fixed rapidity y of the process, the value rapidity taken in BK equation is changed

$$y \rightarrow y - \ln(1 + \frac{4m_q^2}{Q^2}) \quad (7)$$

The form of the function $\tilde{f}(y, k^2, b)$ at initial rapidity, i.e. initial condition for the BK equation Eq.4, has been borrowed from the form of GBW ansatz, [17, 18], with introduced impact parameter dependence. In the paper [4] the following form of the initial conditions for the DIS process on the proton was used

$$\tilde{f}_{proton}(y = y_0, k^2, b) = \frac{3}{4\pi^2} \frac{k^4}{Q_S^2(b)} \exp(-\frac{k^2}{Q_S^2}), \quad (8)$$

where a saturation scale as a function of the impact parameter is defined as following

$$Q_S^2(b) = \frac{S(b)}{C} = \frac{e^{-b^2/R_p^2}}{C\pi R_p^2}. \quad (9)$$

The $S(b)$ function here is the proton impact parameter profile with the usual normalization properties

$$\int S(b) d^2b = 1 \quad (10)$$

and C is a numerical coefficient which defines a value of the saturation scale at zero impact parameter and initial rapidity through the proton radius

$$Q_S^2(b=0) = \frac{1}{C\pi R_p^2}. \quad (11)$$

The generalization of this initial condition for the case of nuclei is straightforward

$$\tilde{f}_{nucleus}(y = y_0, k^2, b) = \frac{3}{4\pi^2} \frac{k^4}{Q_{SA}^2(b)} \exp(-\frac{k^2}{Q_{SA}^2}), \quad (12)$$

where

$$Q_{SA}^2(b) = \frac{AS(b)}{C} \quad (13)$$

with the Wood-Saxon nuclei profile function $S(b)$ for the nucleus with A nucleons which is defined as usual

$$S(b) = \frac{3}{4\pi} \frac{1}{R_A^3 + a^2\pi^2 R_A} \int_{-\infty}^{\infty} \frac{dz}{1 + \exp\left(\frac{-R_A + \sqrt{b^2 + z^2}}{a}\right)} \quad (14)$$

with the parameters

$$R_A = 5.7 A^{1/3} \text{GeV}^{-1}, \quad a = 2.725 \text{GeV}^{-1}. \quad (15)$$

It must be underlined, that the introduced Wood-Saxon nuclei profile Eq. (14) is a attempt of the generalized description of the all nuclei density profiles in one formula. In reality the two parameter Fermi model expression for nuclei density Eq. (14) is mostly applied for heavy nuclei and it is not so correct for the light ones, see [40]. Therefore, the precise consideration of the processes with the light nuclei involved need a introduction of the

$y_0(x_0)$	$R_p^2 (GeV^{-2})$	C	α_s	$m_q^2 (GeV^2)$
3.1 (0.045)	7.9	0.0855	0.108	0.008

Table 1: *The parameters of the model.*

different from the expression Eq. (14) nuclei density profiles and we are not consider this particular task in the paper.

The C parameter in Eq. (13), as well as the value of α_s , value of initial rapidity $y_0(x_0)$ and masses of three light quarks we take the same for the both cases of DIS processes on the proton and nuclei, see Table1. There is a question, is this correct approach to use the same values of the parameters for both processes with the different targets. In principle, due the larger parton densities in the DIS processes on the nuclei, we could expect the differences in the values of α_s and values of y_0 for these two DIS processes. Nevertheless, we must remember that we perform the calculation in the LO and running coupling effects are not directly included in our calculation scheme. We also will see, that a difference in the saturation momenta of the proton and different nuclei is not so large, and , therefore, this difference could not set up the large differences in value of α_s for both processes in the LO calculations. The justification of the use of the same values of α_s and the correctness of used parameters will be shown in the next section, where surprising coincide of our calculations of the integrated gluon density function with the existing parameterizations of the same function will be demonstrated. The same values of the C parameter and value of initial rapidity, from which the evolution equation is valid, may be explained by the same observations. As it seems, these values are more or less universal in the leading order of calculations and shows the physical boundary for the small x evolution independently from the considered target in DIS process.

Last remark which concerns the presented calculations is about the kinematic range of the considered parameters. How it was shown in [4], in the present framework the F_2 HERA data at $Q_0^2 < 1 GeV^2$ could not be described. Therefore, in our calculations we limit the kinematic range of the processes by the $x < x_0$ and $Q^2 > Q_0^2$ constraints. Unfortunately it means, that the main bulk of the data of the DIS on nuclei, [41, 42], is outside of the range aof the applicability of the model, see also remarks above about the form of the nuclei density profile. Therefore, in the next section, we perform the comparison of our results only with the existing parameterizations of the integrated gluon density function , without an introducing of the experimental data fit as it was done in [4].

3 Integrated gluon density function

In [4] was mentioned, that the definition of the integrated gluon density function $xG(x, Q^2)$ through the $\tilde{f}(y, k^2, b)$ function of Eq.3 has ambiguities related with the coupling constant α_s . Indeed, by definition

$$xG(x, Q^2) = \int d^2 b \int^{Q^2} \frac{d k^2}{k^2} f(x, k^2, b) \quad (16)$$

or, in terms of $\tilde{f}(y, k^2, b)$ function

$$xG(x, Q^2) = \int d^2 b \int^{Q^2} \frac{dk^2}{k^2} \frac{\tilde{f}(x, k^2, b)}{\alpha_s(k^2)}. \quad (17)$$

We see from Eq.17 that correct determination of the $xG(x, Q^2)$ function in terms of the $\tilde{f}(x, k^2, b)$ function must include the integration over the running coupling, whereas our calculations scheme includes only LO corrections. In LO approximation the Eq.17 may be redefined as

$$xG(x, Q^2) = \frac{1}{\alpha_s(< Q_{proton}^2 >)} \int d^2 b \int^{Q^2} \frac{dk^2}{k^2} \tilde{f}(x, k^2, b) \quad (18)$$

where the value $\alpha_s(< Q_{proton}^2 >)$ could be considered as a some parameter, which is not necessary the same as in Table1. Similarly, the integrated gluon density function for a nucleus we could write in the following form

$$xG_N(x, Q^2) = \frac{1}{\alpha_s(< Q_{nucleus}^2 >)} \int d^2 b \int^{Q^2} \frac{dk^2}{k^2} \tilde{f}(x, k^2, b), \quad (19)$$

with the $\tilde{f}(y, k^2, b)$ as a solution of corresponding BK equation for DIS process on the nucleus. Our main assumption, which we could check only post priori, is that in LO we could take

$$\alpha_s(< Q_{proton}^2 >) \approx \alpha_s(< Q_{nucleus}^2 >) \quad (20)$$

and, therefore, that the ratio of the integrated gluon densities of the nucleus with A nucleons and the proton

$$R^A(x, Q^2) = \frac{xG_N(x, Q^2)}{A xG(x, Q^2)} \quad (21)$$

does not depend on values of α_s . The first check of the approximation made is simple. We calculate R^A for the following nuclei: gold ($A=197$), neodymium ($A=150$), zinc ($A=70$) and neon ($A=20$) at

$$Q^2 = 2.5, 12, 60, 120 \text{ GeV}^2.$$

Obtained results, see Fig.1, we compare with the calculations of the ratio from the [5, 6, 7, 8], see Fig.2, Fig.3.

As it seems from the Fig.2-Fig.3, in general our results for R^A are in the range defined by curves obtained by the parameterization [6, 7] for R^A ratio, and clearly more differ from the [5, 8] parameterizations of the same ratio. Surprisingly, obtained in absolutely different framework our results somehow interpolate between [6, 7] parameterization of the ratio and stay in the "window" defined at low x by "extremal" parameterizations [5, 8]. The closeness of all curves at the initial point of small x evolution, ($x = 0.045$), shows that we indeed matched the small x evolution of BK equation with the DGLAP framework of [5, 6, 7, 8] in this point. Therefore, this coincidence between the curves from different calculation frameworks indeed justifies the form of used initial conditions for the BK equation and the assumption Eq.20. It is also clear, that all parameterizations [5, 6, 7, 8] are based on the low energy data, whereas the high energy parts of the curves are the extrapolation of the established formulae in the region of small x . This is a explanation for the large differences between the curves from different parameterization in the region of small x in the Fig.2.

Another question is about the parameterization of the nuclei gluon density $xG_N(x, Q^2)$ function in the form

$$xG_N(x, Q^2) = A^{\alpha_A} xG(x, Q^2) \quad (22)$$

where is the coefficient α_A (do not be confused with the coupling constant α_s) determines the "power" of the shadowing for each nucleus at different Q^2 . In spite of the parameterization based on the data fitting, in our approach this coefficient is calculable, see also [23] for the similar calculations. The results of the calculation of the α_A coefficient is presented in the Fig.4. From Fig.4 it is clear, that the obtained shadowing is weaker than usually obtained in the framework of BK equation, see again paper [23] for example.

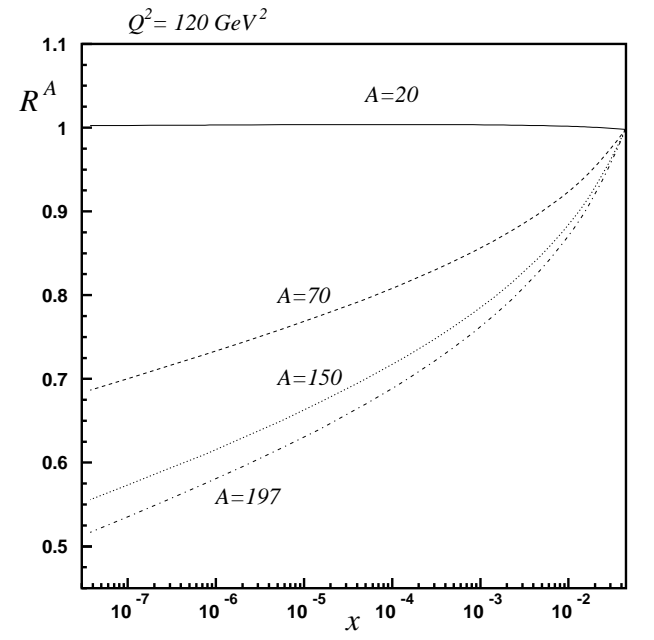
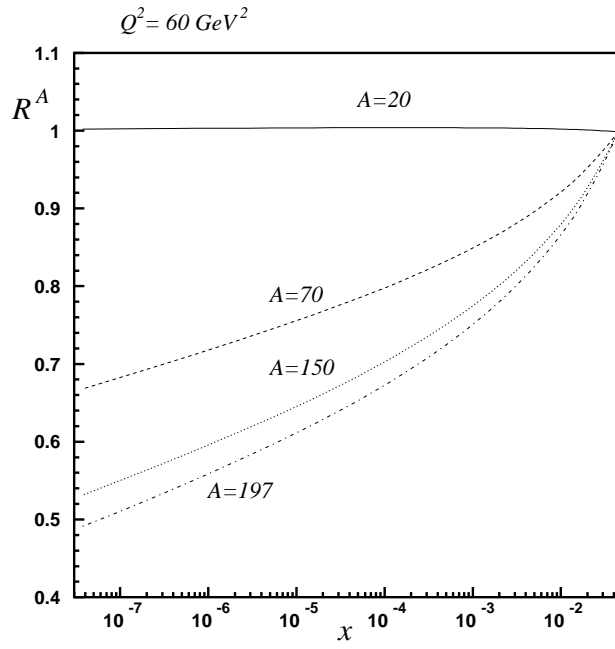
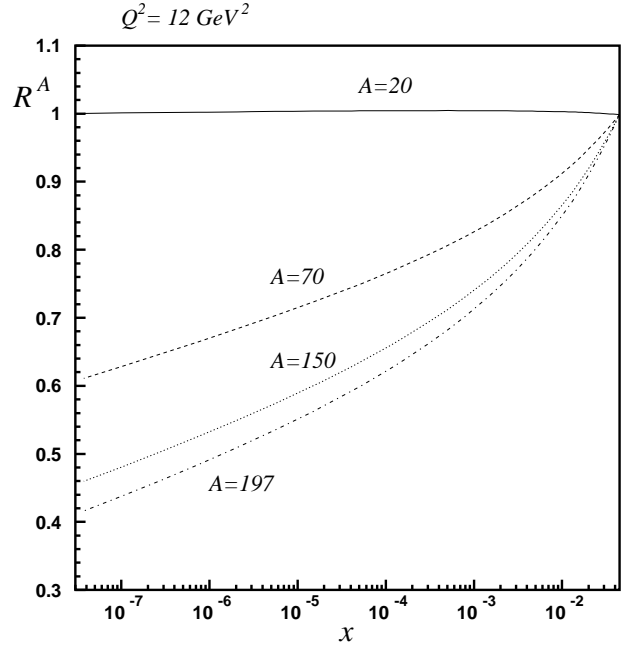
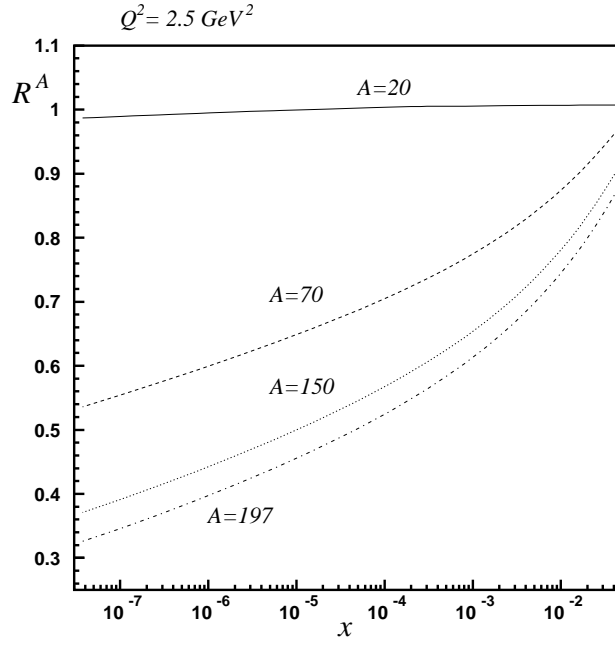


Figure 1: The ratio $R^A(x, Q^2)$ for different nuclei at different Q^2 .

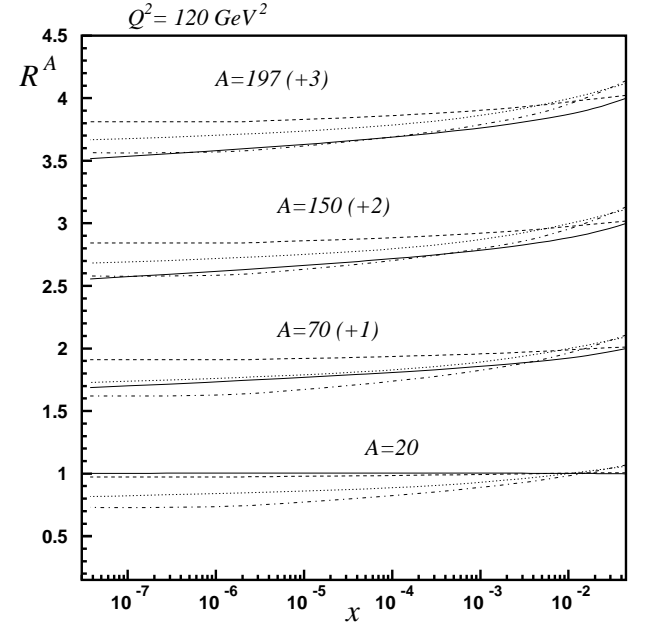
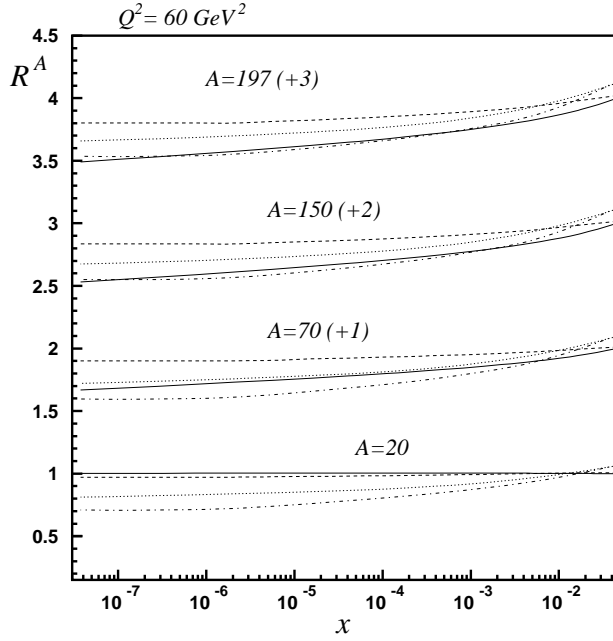
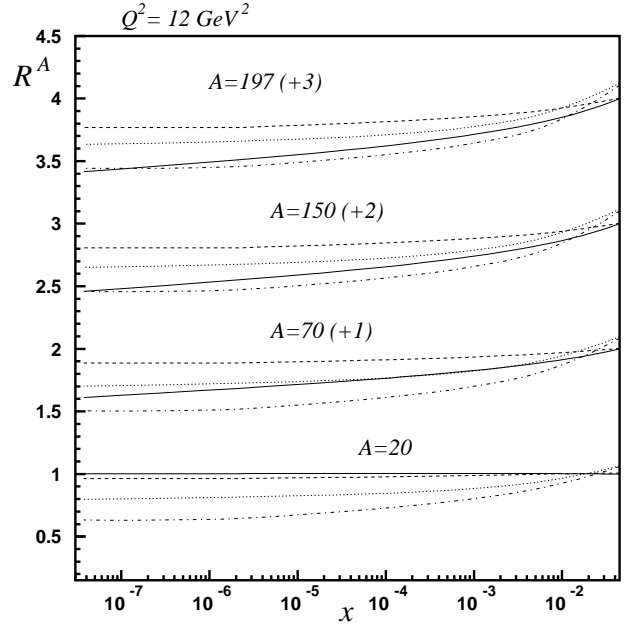
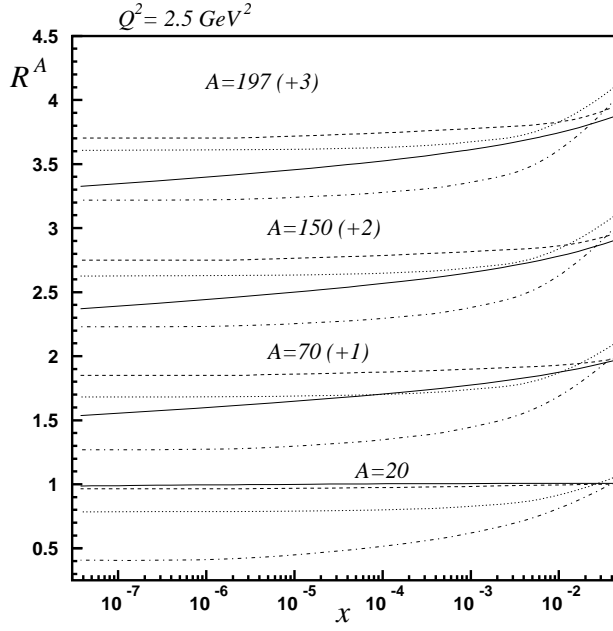


Figure 2: The ratio $R^A(x, Q^2)$ of integrated gluon density functions: the present model results (solid lines), the results from [5] (dashed lines), the results from [6] (dotted lines) and the results from [7] (dashed-dotted lines). The numbers in brackets show the added number to the real value of R^A .

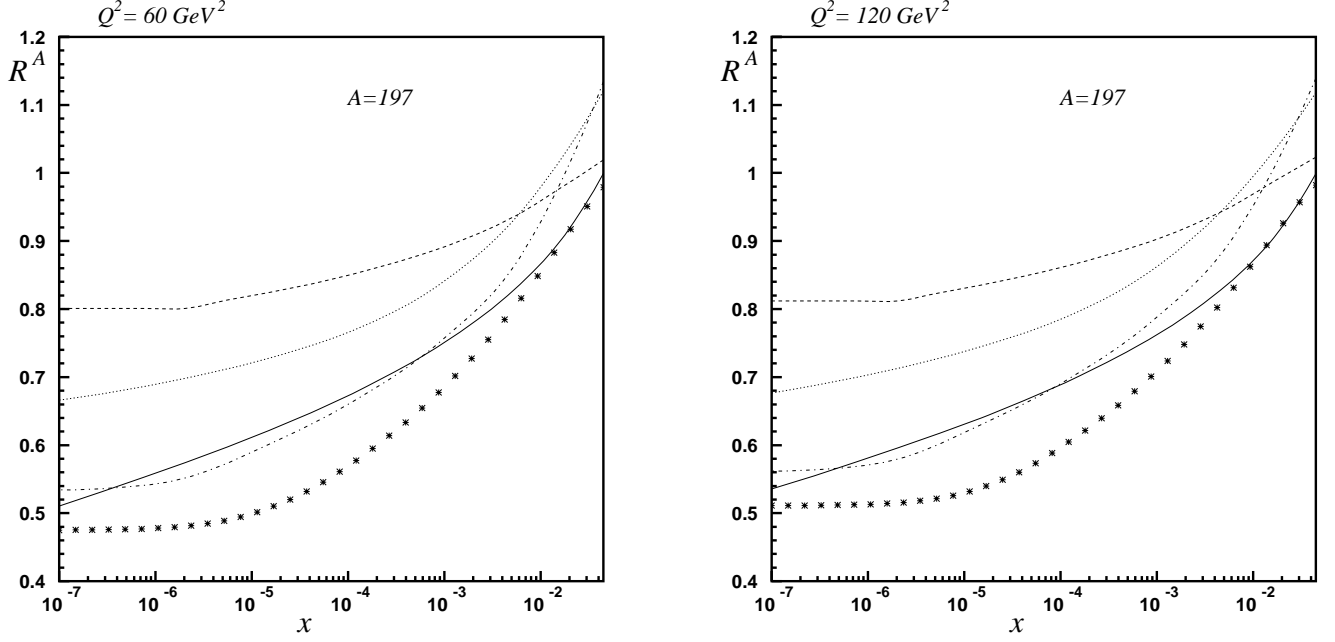


Figure 3: The ratio $R^A(x, Q^2)$ of integrated gluon density functions for the DIS on the gold at $Q^2 = 60, 120 \text{ GeV}^{-2}$: the present model results (solid lines), the results from [5] (dashed lines), the results from [6] (dotted lines), the results from [7] (dashed-dotted lines) and the results from [8] (stars).

4 F_2 structure function

Using usual definition of F_2 structure function

$$F_2(x, Q^2) = \frac{Q^2 \alpha_s}{4 \pi^2 \alpha} \int d^2 b \int \frac{d^2 k}{k^4} \frac{f(x, k^2, b)}{4 \pi} (\Phi_T(k, m_q^2) + \Phi_L(k, m_q^2)) \quad (23)$$

we obtain the same expression in terms of $\tilde{f}(y, k^2, b)$ unintegrated gluon density function

$$F_2(x, Q^2) = \frac{Q^2}{4 \pi^2 \alpha} \int d^2 b \int \frac{d^2 k}{k^4} \frac{\tilde{f}(x, k^2, b)}{4 \pi} (\Phi_T(k, m_q^2) + \Phi_L(k, m_q^2)) . \quad (24)$$

The expressions for the impact factors in Eq.23-Eq.24 are given in Eq.5-Eq.6. There the α_s coupling constant is excluded from the expression comparing to the usual definition of the impact factors, that allows to write Eq.24 in the way where formally α_s is not appeared in the expression. As in the previous case of integrated gluon density function, the main object of our interest is a ratio of the nucleus and proton structure functions

$$R_{F_2}^A = \frac{F_{2N}(x, Q^2)}{A F_2(x, Q^2)} . \quad (25)$$

The results for this ratio are presented in the Fig.5. Comparing the result of the Fig.1 with the results presented in the Fig.5 it is easy to see, that in contrary to the $xG_N(x, Q^2)$ function the structure function $F_{2N}(x, Q^2)$ does not proportional to the $A F_2(x, Q^2)$ even at high x . Introducing the following parameterization

$$F_{2N}(x, Q^2) = A^{\beta_A} F_2(x, Q^2) \quad (26)$$

we obtain for the coefficient β_A results which presented in the Fig. 6. As it seems from the Fig.6 the coefficient

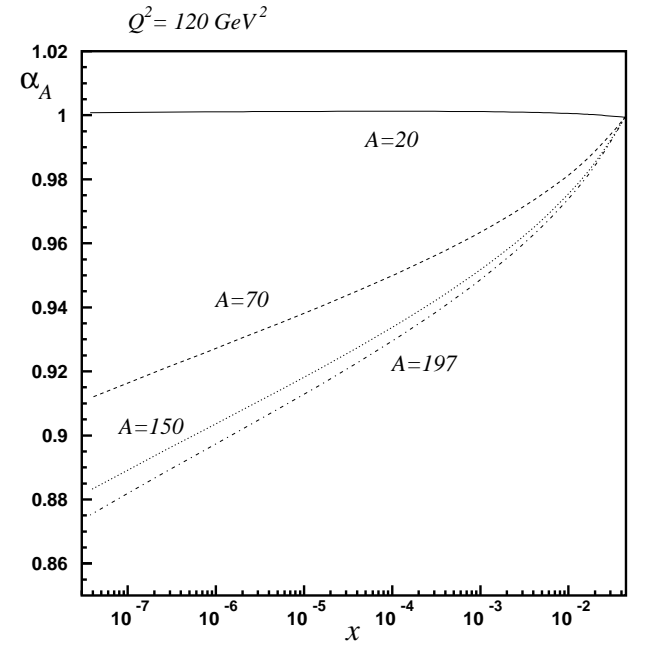
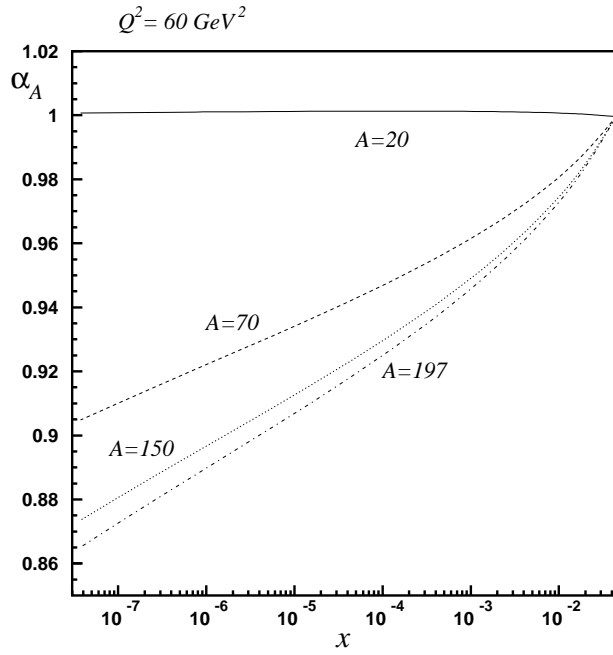
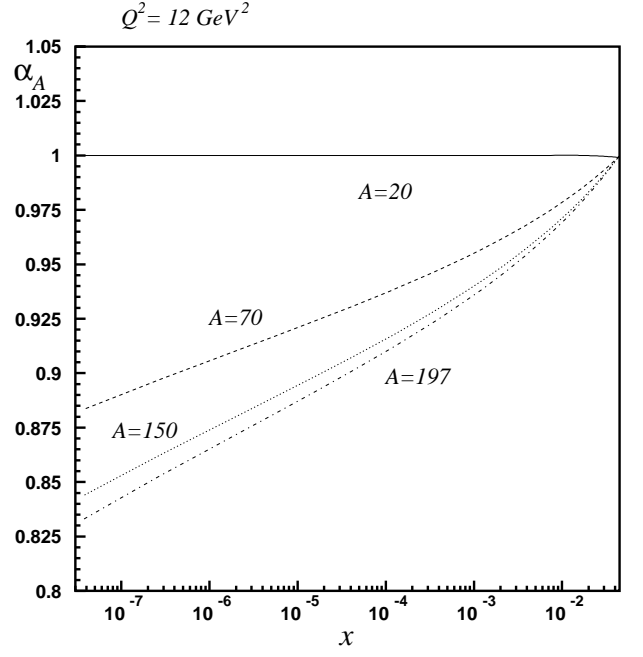
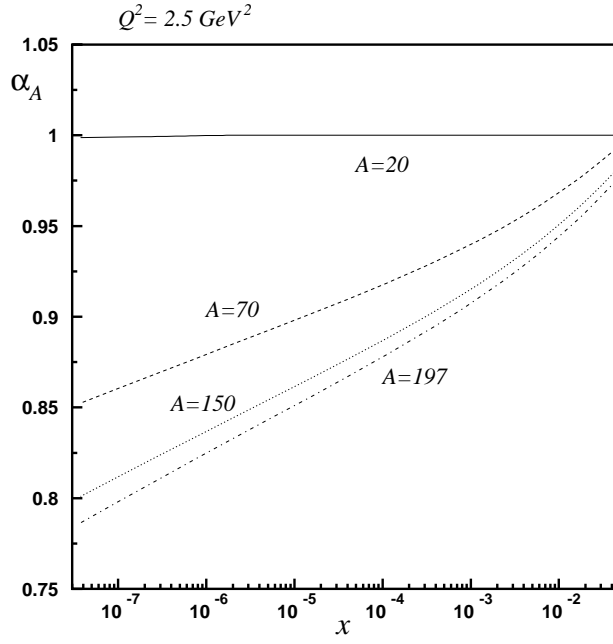


Figure 4: The α_A coefficient of Eq.22 for different nuclei at different Q^2 .

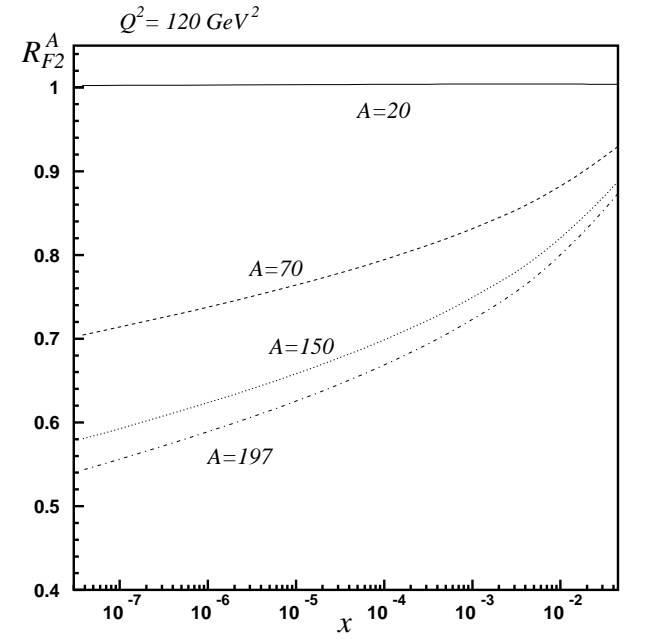
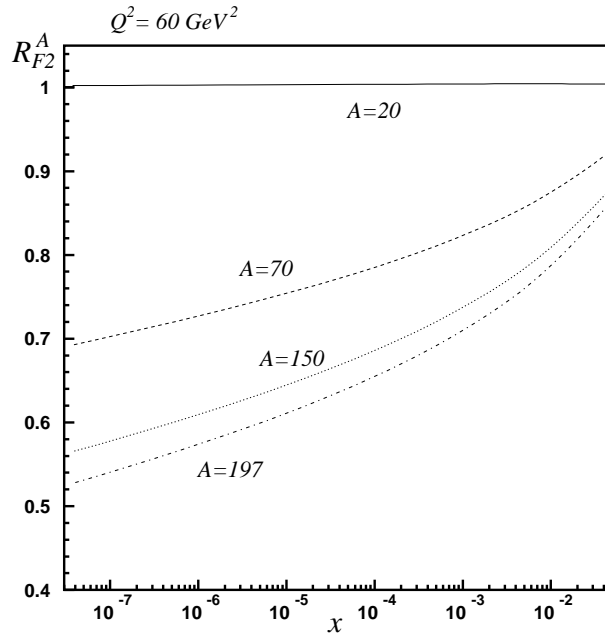
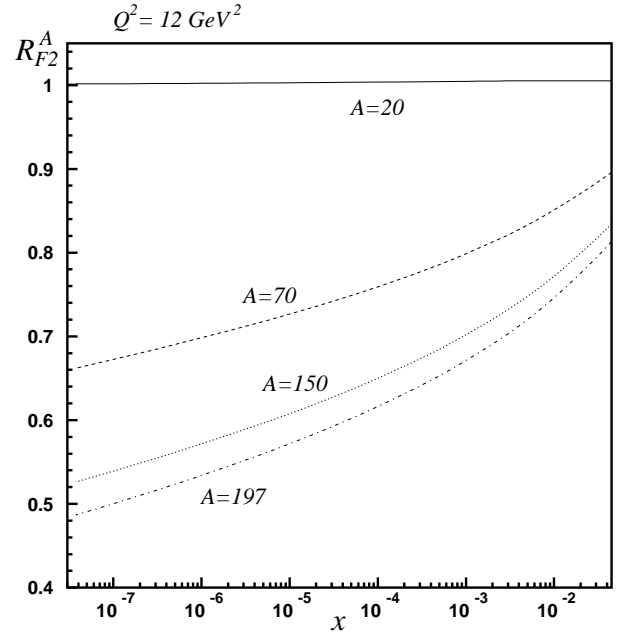
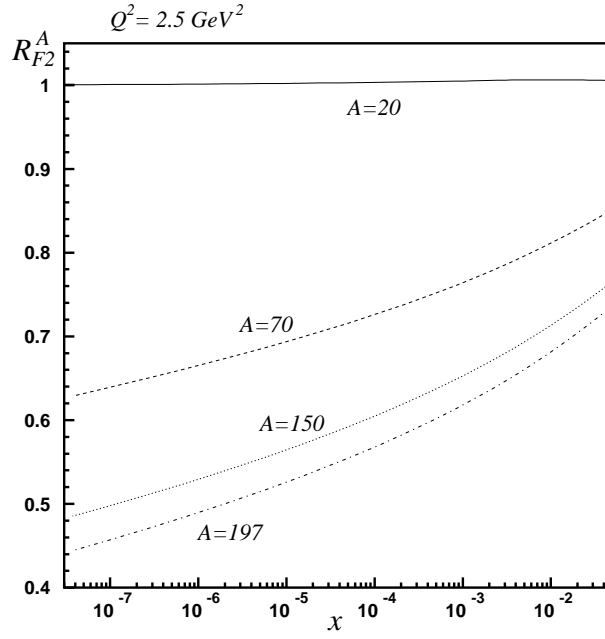


Figure 5: The R_{F2}^A ration for different nuclei at different Q^2 .

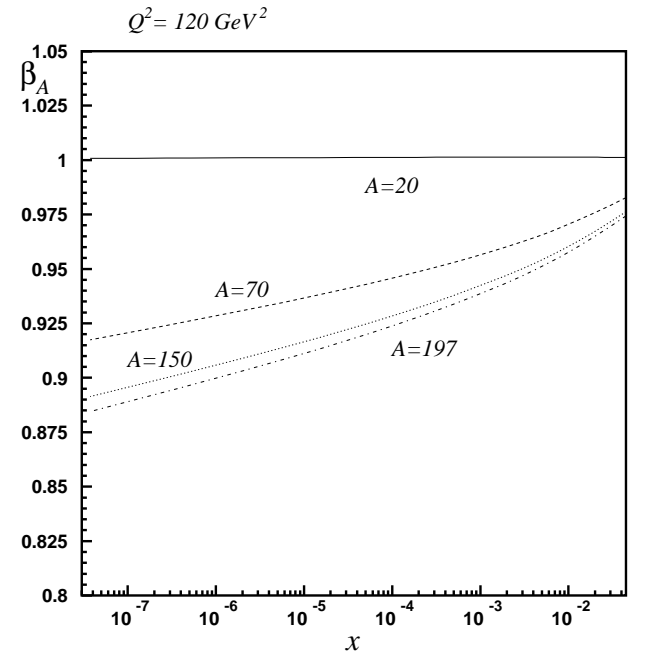
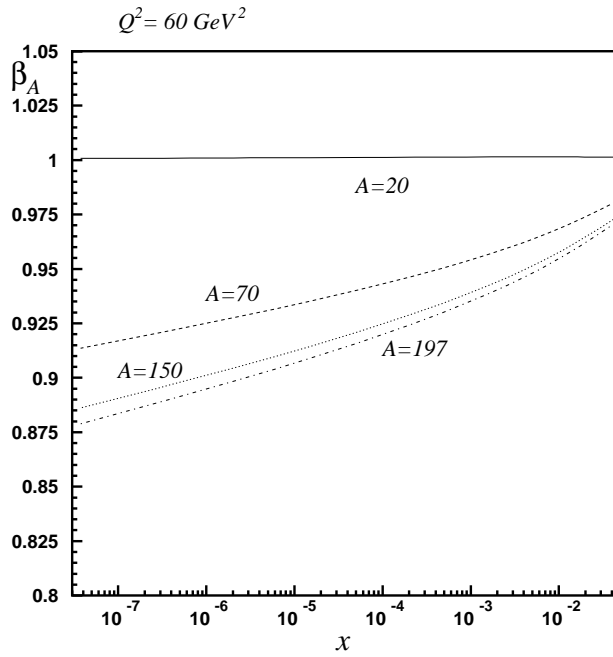
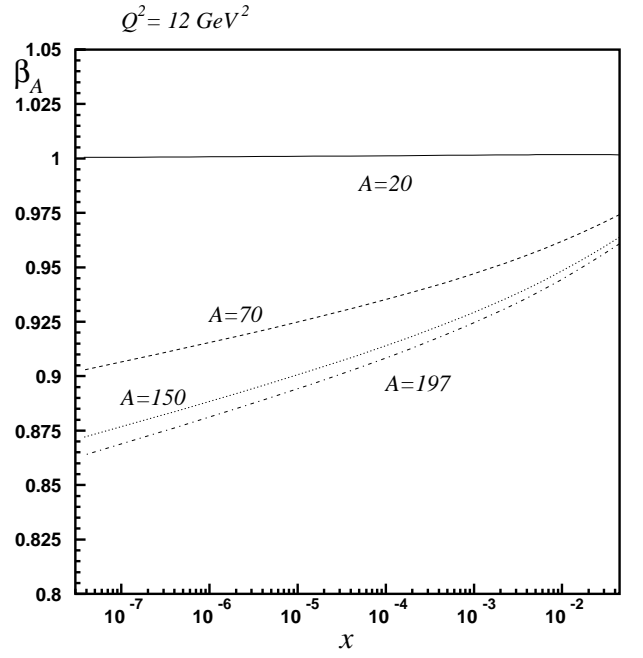
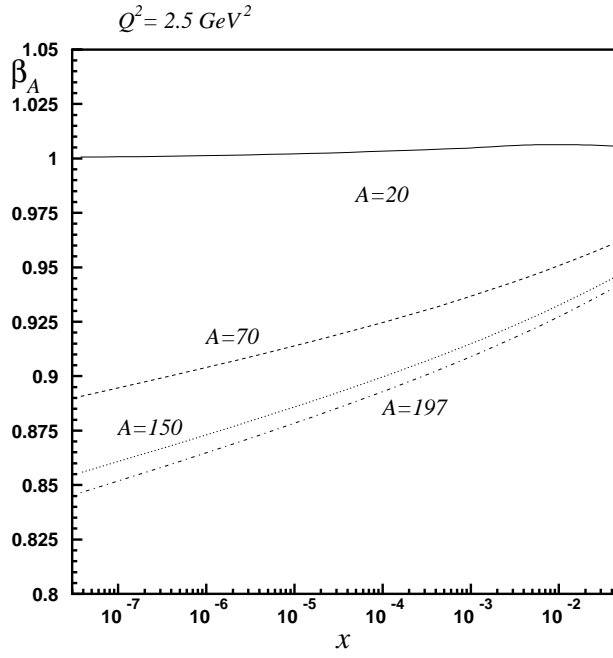


Figure 6: The β_A coefficient of Eq.26 for different nuclei at different Q^2 .

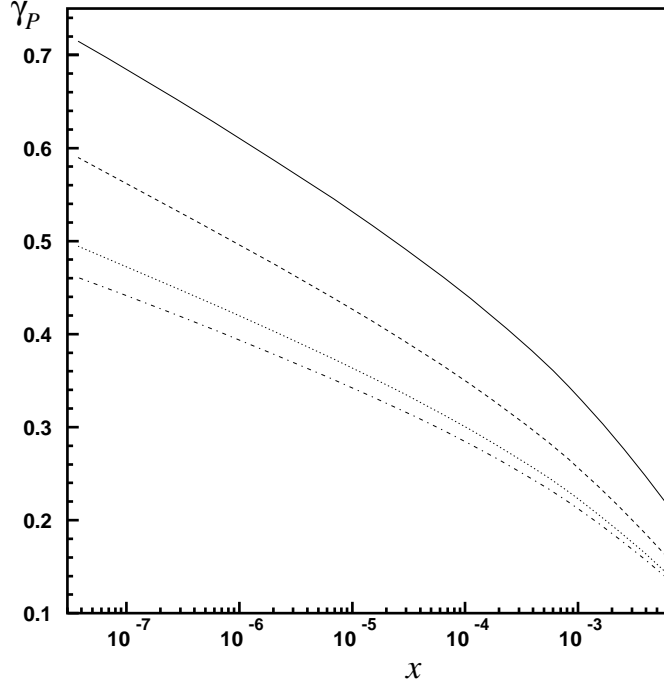


Figure 7: Anomalous dimension γ for the case of DIS on the proton at different Q^2 : $Q^2 = 2.5 \text{ GeV}^2$ (solid line), $Q^2 = 12 \text{ GeV}^2$ (dashed line), $Q^2 = 60 \text{ GeV}^2$ (dotted line), $Q^2 = 120 \text{ GeV}^2$ (dashed-dotted line).

β_A is less sensitive to the details of the process, i.e. to the values of Q^2 and type of the nucleus than α_A coefficient from Fig.5. It is also interesting to note, that even at high values of x the coefficient β_A does not equal to one, in contrary to the α_A .

5 Anomalous dimension

Let's consider the definition of the average anomalous dimension γ in DIS process via the integrated gluon density function

$$xG(x, Q^2) \propto (Q^2)^\gamma \quad (27)$$

see [36]. In this case the calculation of γ is straightforward

$$\gamma = \frac{\partial \ln (xG(x, Q^2))}{\partial \ln Q^2} \quad (28)$$

The result for γ for the case of DIS process on the proton is represented in Fig.7 and for the case of DIS on the nuclei in the Fig.8. Considering the γ_P anomalous dimension from the Fig.7, it is interesting to note, that for DIS process on the proton at $Q^2 > 60 \text{ GeV}^2$ the value of γ_P is below the value of BFKL anomalous dimension $\gamma_{BFKL} \approx 0.5$ at whole range of x . At small values of Q^2 the γ_P value is about BFKL 0.5 already at $x \propto 10^{-4} - 10^{-5}$, that one more time underline the importance of rescattering correction (shadowing corrections) in this kinematic region. From the result of the calculations of anomalous dimension for the different nuclei γ_A in Fig.8 we see, that in contrary to the calculations of [23] the γ_A shows clear dependence

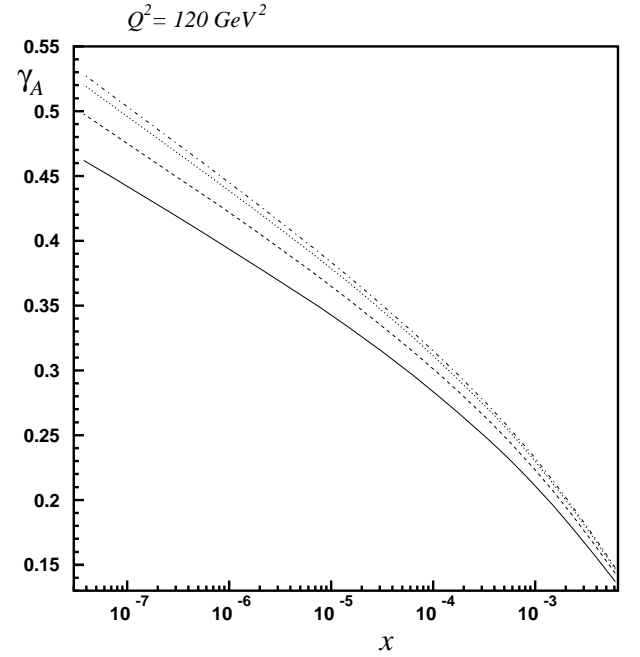
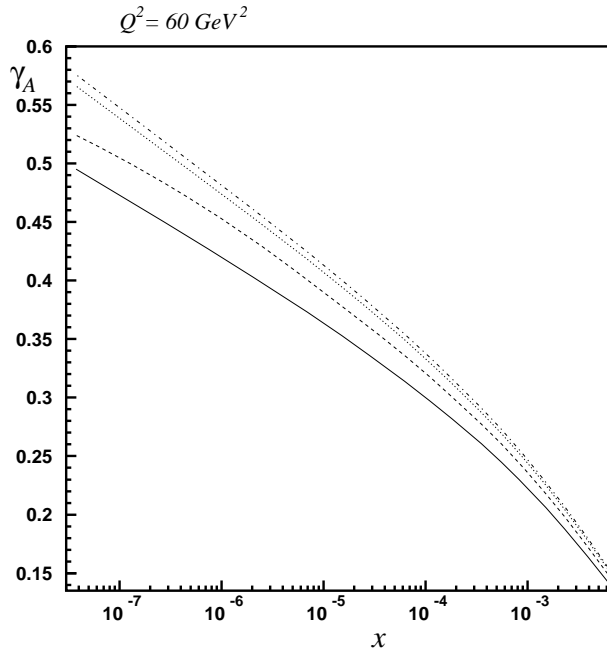
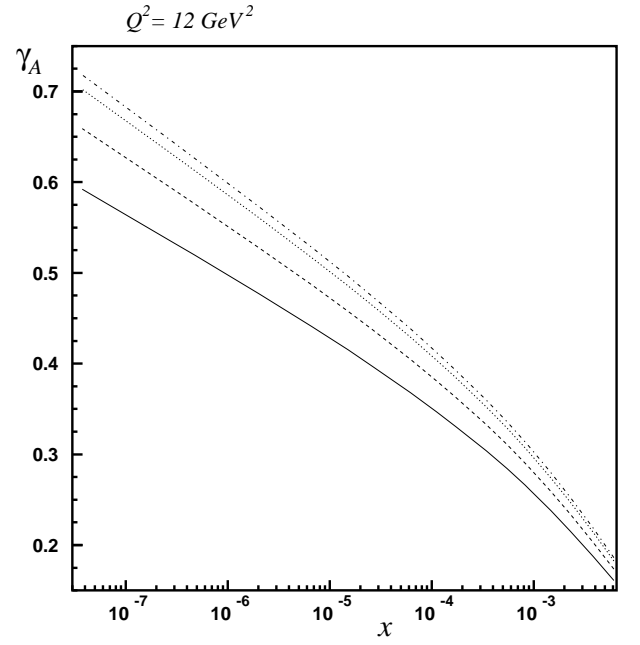
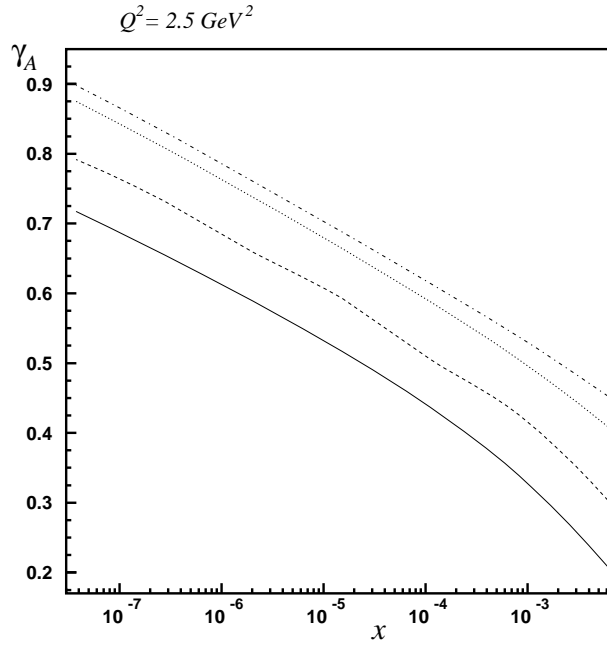


Figure 8: Anomalous dimension γ for the case of DIS on the nuclei: $A=20$ (solid line), $A=70$ (dashed line), $A=150$ (dotted line), $A=197$ (dashed-dotted line).

on the atomic number A at all values of Q^2 at small $x < 10^{-4}$. Decrease of the value of Q^2 in the DIS process leads to the increase of the value of γ_A , that indicates the increasing of value of the shadowing corrections in the process.

6 Saturation momenta

There are different definitions of the saturation momenta, which are used through the literature about the subject. For example, in papers [23] the saturation momenta in DIS process was defined with the help of a packing factor $\kappa_p(Q^2, x)$. As a saturation momenta there was considered a momenta where

$$\kappa_p(Q_S^2, x) = 1/2 \quad (29)$$

at fixed x and impact parameter (if, of course, the impact parameter is introduced in definition of $\kappa_p(Q^2, x)$). In our paper we use a different definition of saturation momenta, borrowed from [37]. Following the definition of [37] we define a saturation momenta as a momenta where a maximum of the unintegrated gluon density function is reached at fixed impact parameter and fixed x :

$$Q_S(b, x) : \frac{\tilde{f}(x, Q_S, b)}{k^2} > \frac{\tilde{f}(x, k, b)}{k^2} \text{ for any } k : k_{min} < k < k_{max}, \quad (30)$$

where k_{min} and k_{max} are correspondingly minimum and maximum momenta used in numerical calculations. This $Q_S^2(b)$ definitely depends on impact parameter and, in fact, may be used in order to introduce the impact parameter dependence in the scaling solution of usual BK equation. In the next subsections we will use the definition Eq.30 for the calculations of saturation momenta of the proton and different nuclei.

6.1 Saturation momenta for DIS process on the proton

Plot of the saturation momenta of the proton, defined through the Eq.30, are presented in the Fig.9-Fig.10. Considering the saturation momenta at fixed impact parameters, we could write a very simple expression for the approximate parameterization of the saturation momenta of the proton

$$Q_S^2(b, x) = Q_{S0}^2(b) + Q_{S1}^2(b) \left(\frac{x_0}{x} \right)^{d(b)}, \quad (31)$$

where the coefficients $Q_{S0}^2(b)$, $Q_{S1}^2(b)$ and $d(b)$ in this parameterization could be extracted from the Fig.9 data. The fitting procedure for the data in the range of x such that $x = 1.66 \cdot 10^{-2} - 3.75 \cdot 10^{-8}$ gives the following values of coefficients

$$Q_S^2(b, x) = F_S(x) S(b) = \left(8.69 + 12.65 \left(\frac{10^{-7}}{x} \right)^{0.46} \right) \frac{e^{-b^2/R_p^2}}{\pi R_p^2} \text{ GeV}^2, \quad (32)$$

with the coefficient d which does not dependent on impact parameter and with the proton radius from the Table 1. Comparing the expression of the saturation momenta Eq.32 with the coefficient C from the expression Eq.9, we see, that the expression Eq.32 gives $C = 0.11 \text{ GeV}^2$ instead $C = 0.0855 \text{ GeV}^2$ in initial conditions Eq.9. The difference between these two values is due the "averaging" procedure used in fitting the data. The expression Eq.32 is the result of fitting of many points, and there is not necessary that the resulting curve will cross precisely the initial point in the fitted data. Obtained value of the coefficient $d = 0.46$ is close to the results of [37]. We obtained $c = 2.2$ instead $c = 2.06$ in the terms of the paper [37]. From the Eq. (32) and

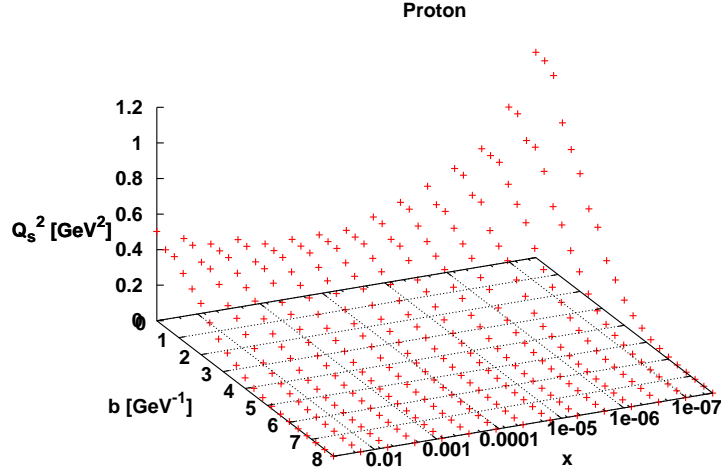


Figure 9: Saturation momenta of the proton as a function of x and impact parameter.

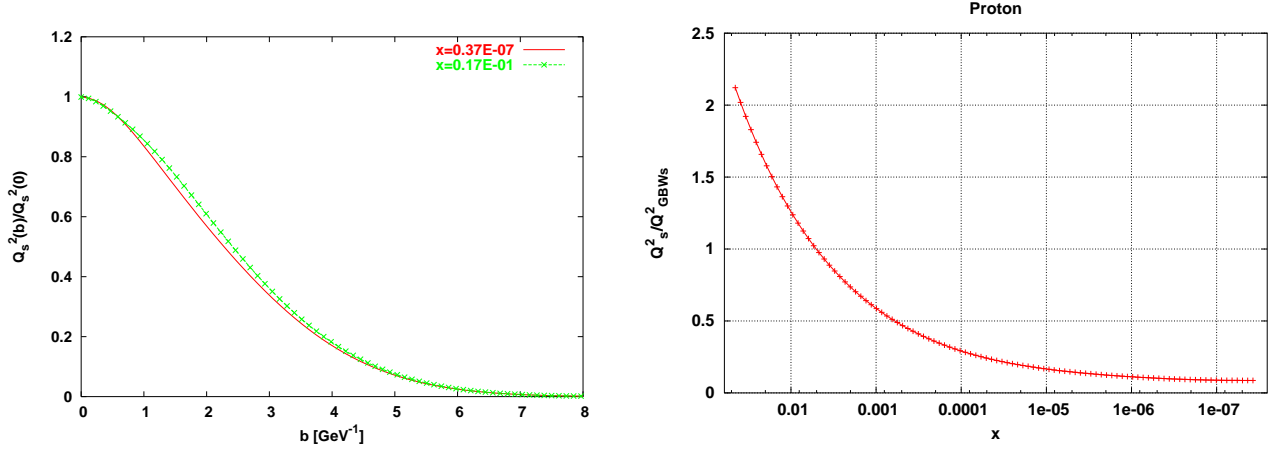


Figure 10: Saturation momenta as a function of impact parameter at fixed values of x in the left plot and the comparison of the obtained saturation momenta at $b = 0$ with the GBW saturation momenta from the [17] in the right plot of the picture.

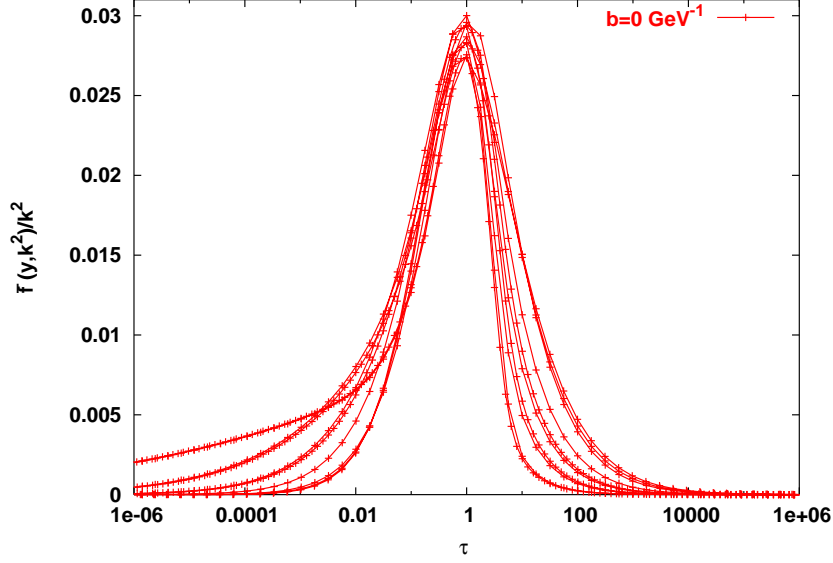


Figure 11: Unintegrated gluon density function $\tilde{f}(x, k^2, b) / k^2$ as a function of scaling variable τ at $b = 0$ and different $x = 6.1 \cdot 10^{-3} - 3.8 \cdot 10^{-8}$ (curves from up to down in the left half of the plot) for the case of DIS on the proton.

Fig.10 we see, that our answer for the saturation momenta is different from the obtained in the GBW model [17]. We will discuss these differences in the conclusion of the paper.

With the help of $Q_S^2(b, x)$ it is easy to investigate scaling properties of the unintegrated gluon density function $\tilde{f}(y, k^2, b)$. Plotting $\tilde{f}(x, k^2, b) / k^2$ as a function of only $\tau = \frac{k^2}{Q_S^2(b, x)}$ at $b = 0$, we obtain results presented in the Fig.11. As it seems from the Fig.11, the only approximate scaling of $\tilde{f}(x, k^2, b) / k^2$ exists, if we collect all the data at different values of x . This approximate scaling behavior is mostly pronounced near the maximum of the $\tilde{f}(x, k^2, b) / k^2$ function and it is clearly broken in the "tails" of the function at large and small values of τ . Nevertheless, if we consider the $\tilde{f}(x, k^2, b) / k^2$ at fixed x and at different b , then we see a perfect scaling behavior of the function, see Fig.12. The only approximation scaling behavior of the unintegrated gluon density means, that $\tilde{f}(x, k^2, b) / k^2$ is likely a function of two variable, i.e. that $\tilde{f}(x, k^2, b) / k^2 = F(x, \tau(x, b))$ in the given framework.

6.2 Saturation momenta for DIS process on the nuclei

The behavior of the saturation momenta of the different nuclei as a function of impact parameter and x is presented in the Fig.13 and in the left plot of the Fig.14. We parametrize the saturation momenta of the nuclei in the following form

$$Q_{SA}^2(b, x) = Q_{S0A}^2(b) + Q_{S1A}^2(b) \left(\frac{x_0}{x} \right)^{d(b)}. \quad (33)$$

The fitting of the data gives the following expression for the saturation momenta of the nuclei

$$Q_{SA}^2(b, x) = F_{SA}(x) A S(b) = \left(8.84 + 12.56 \left(\frac{10^{-7}}{x} \right)^{0.46} \right) A S(b) \text{ GeV}^2, \quad (34)$$

where $S(b)$ is a Wood-Saxon nuclei profile function from Eq.14. We see, that the coefficients in the $F_S(x)$ function in Eq.34 are the same as in the expression for the saturation momenta of the proton in Eq.32. Indeed,

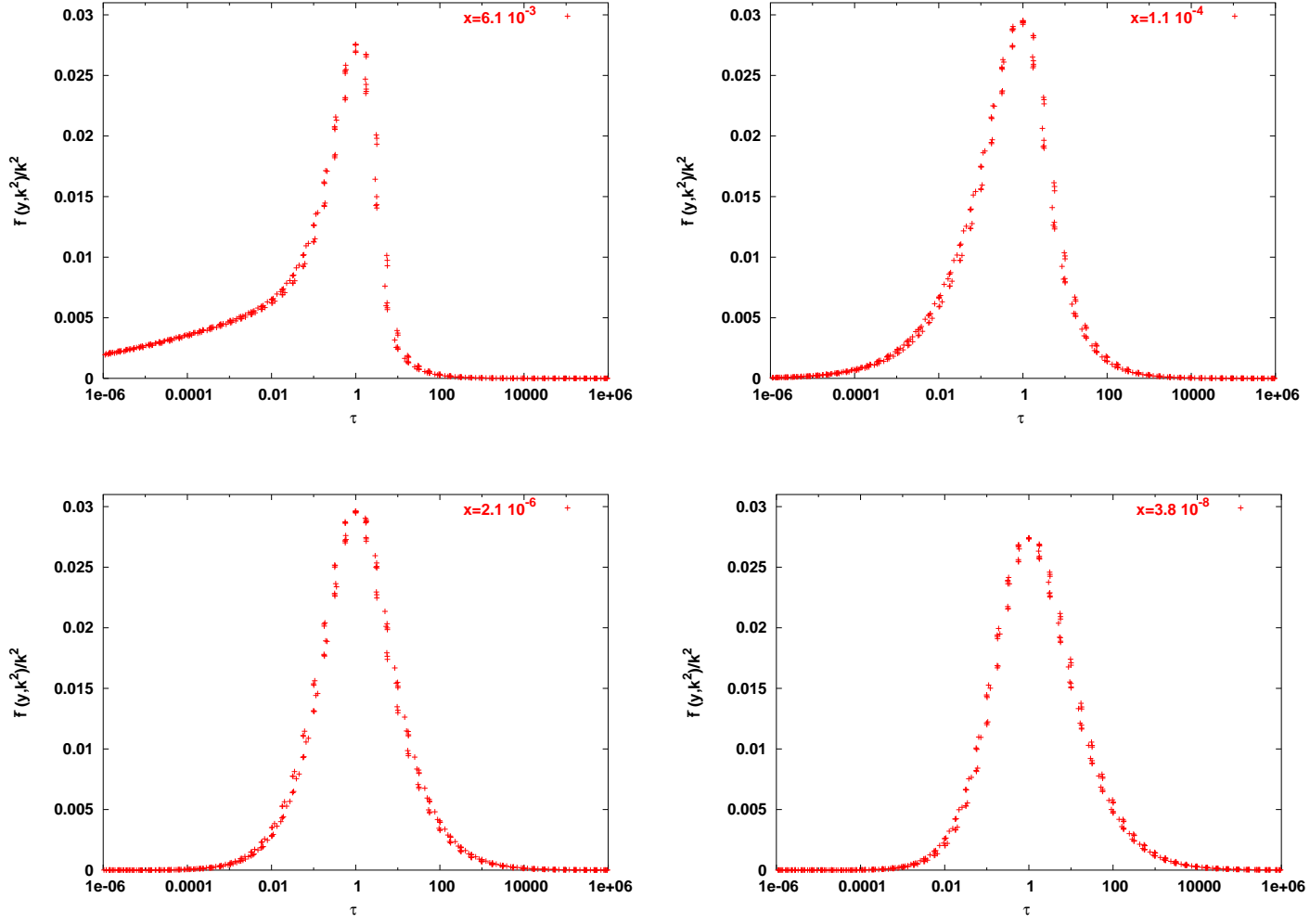


Figure 12: Unintegrated gluon density function $\tilde{f}(x, k^2, b) / k^2$ as a function of scaling variable τ at fixed values of x and different $b = 0 - 12 \text{ GeV}^{-1}$ for the case of DIS on the proton.

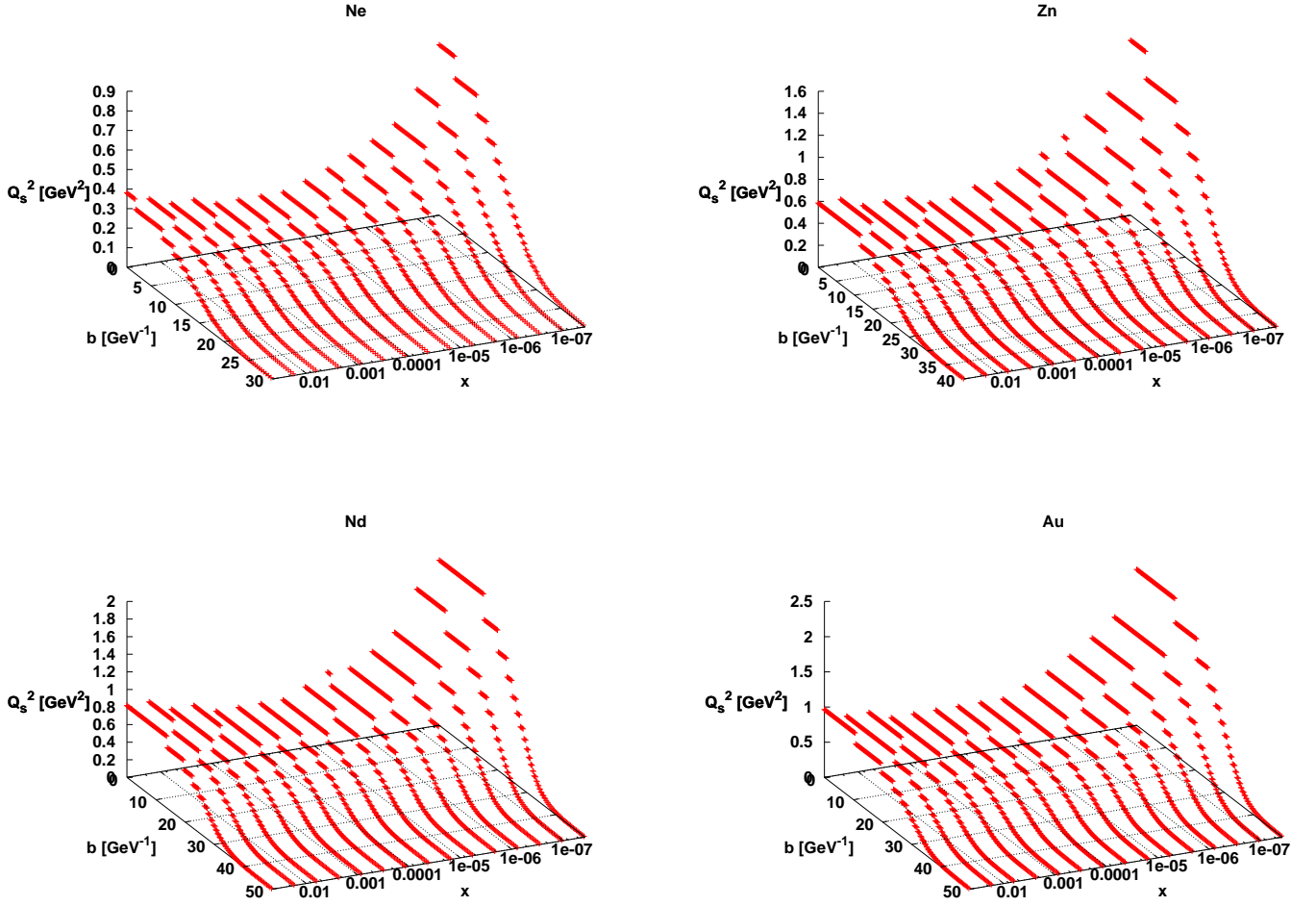


Figure 13: *Saturation momenta of nuclei as a function of x and impact parameter.*

if we compare the expression Eq.34 with the Eq.13 we see, that the coefficient C from Eq.13 must be the same as in Eq.9. Therefore, apart the impact parameter dependence and number of nucleons in target, the expressions for saturation momenta in Eq.32 and Eq.34 are the same.

Now we could compare the expression Eq. (32) and Eq. (34). It is easy to see the following relation between saturation scales

$$Q_{SA}^2(0, x) \approx \frac{Q_S^2(0, x) A S_A(0)}{S_p(0)}, \quad (35)$$

where $S_A(0)$ and $S_p(0)$ are the proton and nuclei profile functions correspondingly. So, from our expressions for the saturation momenta we obtain

$$\frac{Q_{SA}^2(0, x) S_p(0)}{Q_S^2(0, x) A S_A(0)} \approx 1. \quad (36)$$

The independent calculations of this ratio presented in the right plot of the Fig.14 shows that the expression Eq. (36) is indeed correct. Now it is easy to obtain a A^n behavior of the nuclei saturation momenta. Having in mind that

$$\frac{A S_A(b)}{S_p(b)} = A^{1/3} k_A(b) \quad (37)$$

we obtain

$$Q_{SA}^2(b, x) = A^{1/3} k_A(b) Q_S^2(b, x). \quad (38)$$

We see, that we obtained a usual DGLAP $A^{1/3}$ dependence of the nuclei saturation momenta with the additional modification coefficient $k_A(b)$ which arises due the different sizes of proton and nuclei and which depend on the atomic number A of the nuclei. In the case of the considered nuclei this coefficient varies as $k_A(0) = 0.28 - 0.34$. The DGLAP $A^{1/3}$ dependence in Eq. (38) again underline the relative smallness of the shadowing effects in the processes of interest. We also note, that $k_A(b)$ coefficient is related with the diluteness parameter κ_A from [27]

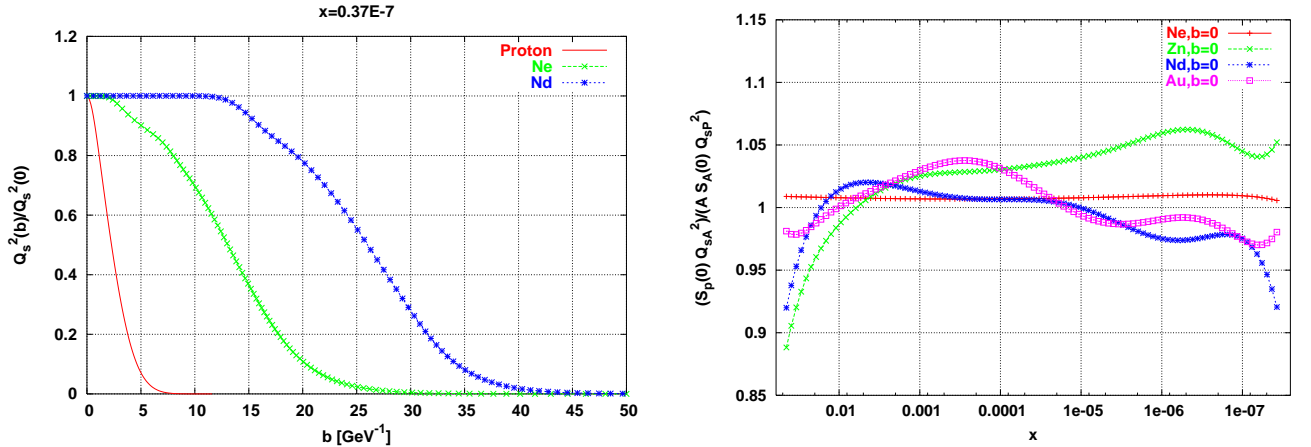


Figure 14: *Normalized impact parameter profile of the saturation momenta of the proton and different nuclei in the left plot of the picture and ratio Eq.36 for the different nuclei in the right plot of the picture.*

which is defined as

$$\kappa_A(b) = A^{1/3} k_A(b). \quad (39)$$

For the considered nuclei this parameter varies as $\kappa_A(0) = 0.76 - 2$ that support the point of view of [27] on the nucleus as on the pretty dilute system of nucleons.

Investigating the scaling properties of the nuclei unintegrated gluon density function in the same way as it was done before for the proton case and again introducing the $\tau = \frac{k^2}{Q_s^2(b,x)}$ variable we obtain results shown in the Fig.15. As in the case of the DIS on the proton we see, that the scaling is precise only at fixed value of

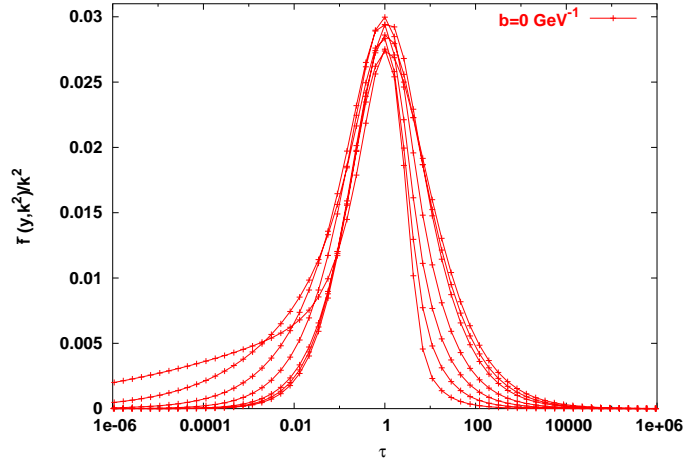


Figure 15: Unintegrated gluon density function $\tilde{f}(x, k^2, b) / k^2$ as a function of scaling variable τ at $b = 0$ and different $x = 6.1 \cdot 10^{-3} - 3.8 \cdot 10^{-8}$ (curves from up to down in the left half of the plot) for the case of DIS on the gold ($A = 197$).

x. In general, the scaling behavior of the unintegrated gluon density function is only approximation, see again Fig.15 and Fig.16.

7 Conclusion

As the main result of this paper we consider the application of the BK evolution equation with the local impact parameter dependence to the DIS processes on the nuclei at small values of Bjorken x with the initial conditions of the rapidity evolution similar to the usual GBW ansatz. The precise form of the initial conditions for the case of DIS on the proton was obtained in the paper [4] with the help of F_2 HERA data fit and we considered a DIS process on the nuclei using the same functional form of the initial conditions. Definitely, it is not fully clear why the main parameters of the initial conditions will not be changed if the processes with nuclei instead the proton are considered. Nevertheless, surprisingly, in the given framework we obtained the integrated gluon density function which similar to the integrated gluon density functions from the known parameterizations in the initial point of evolution, see Fig.2-Fig.3. The explanation of this fact is very simple, in the given framework the conditions for the applicability of high energy formalism seems to be universal. Indeed, let's consider the α_s coupling as a parameter which defines a physical "condition" of the process. We assume, that the value of α_s is determined by some averaged saturation momenta. In considered range of x , $x = 4.5 \cdot 10^{-2} - 3.8 \cdot 10^{-8}$, the value of saturated momenta and, correspondingly the value of α_s is almost the same for the proton and nuclei in LO calculation scheme. It gives a physical explanation of this universality, the application of the BFKL and BK equations in DIS process is independent on the considered target of the process.

It was mentioned above, that the interesting property of the obtained results for the integrated gluon density function is that it stays in the range of the results for the integrated gluon density functions obtained

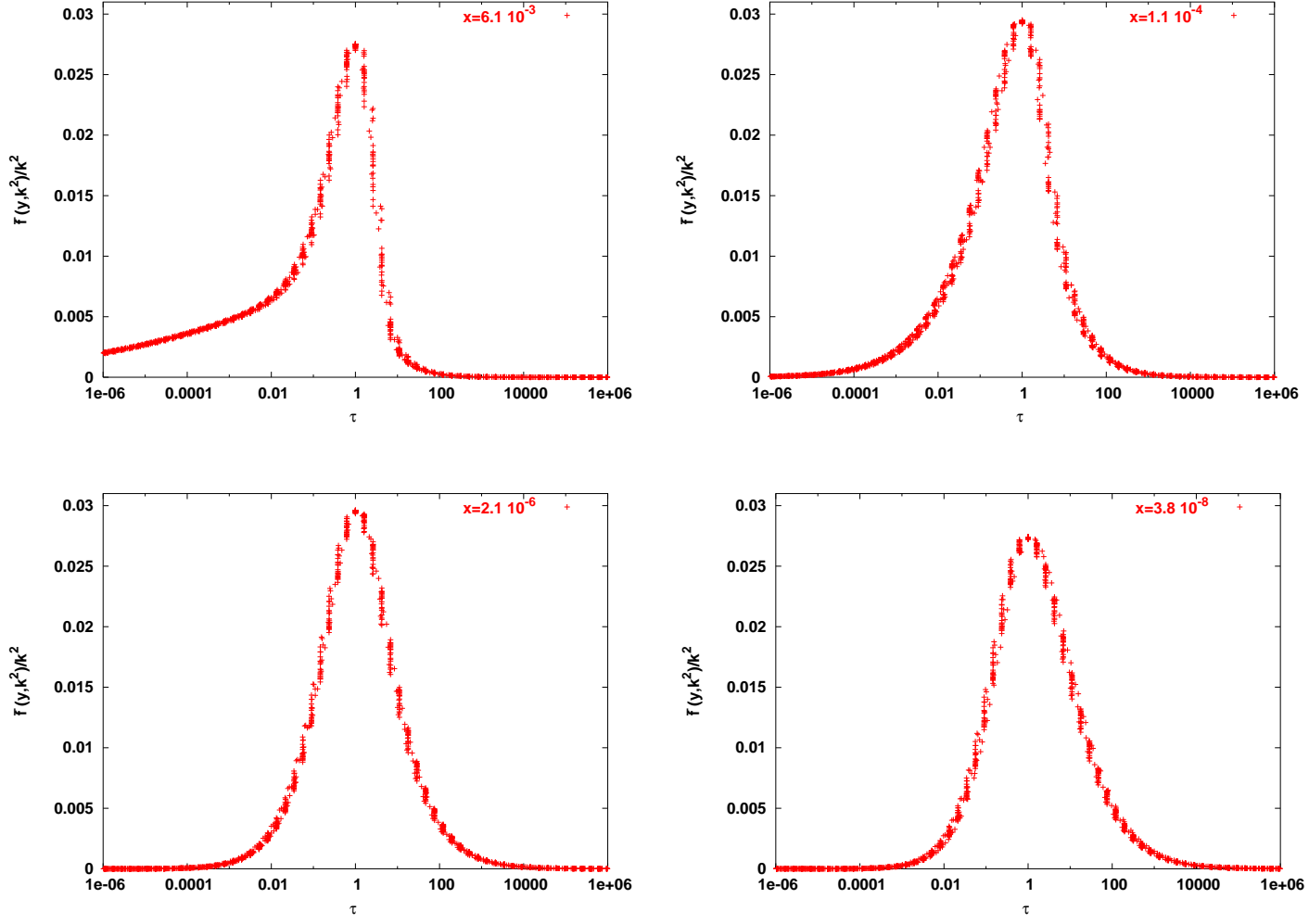


Figure 16: *Unintegrated gluon density function $\tilde{f}(x, k^2, b) / k^2$ as a function of scaling variable τ at fixed values of x and different $b = 0 - 110 \text{ GeV}^{-1}$ for the case of DIS on the gold ($A = 197$).*

in the different parameterization schemes which base on the application of DGLAP equation to the low energy experimental data, see again Fig.2-Fig.3. This fact, justifying chosen form of the initial conditions, causes a interesting question. In general, there is no physical reason why the curves obtained in framework of BK equation will be the same as the curves obtained in the DGLAP calculation scheme. Clearly, first of all, the reason for the such behavior of the curves is that the LO BFKL equation defines the same behavior for the integrated gluon density function as the LO DGLAP equation in some kinematic ranges. At large values of Q^2 , when BK triple Pomeron vertex corrections are small, the coincidence of the curves is a sequence of this fact. More interesting, that the curves obtained in BK equation formalism are still pretty close to the other curves at smaller values of Q^2 . As a explanation of this we assume that the triple Pomeron vertex corrections are relatively small in the considered kinematic range of x and Q^2 . As it seems, at given Q^2 and x the contribution of these corrections is not large, that makes resulting curves based on the BK and DGLAP equations formalism to be similar. Going into the region of smaller Q^2 at the small given and fixed values of x , we will see a larger deviations between the results. At very small values of Q^2 the considered LO BK equation fails to describe data, that could be a sign not only of a significance of the triple Pomeron vertex corrections but also a sign of the need to add a further, "net" diagrams corrections into the process, see [4, 11, 12, 15, 38, 39]. Of course, going into the region of smaller x at fixed values of Q^2 , we also will obtain the more significant deviation between the curves of different approaches caused by the large triple Pomeron vertex corrections.

The additional mark of the smallness of the triple Pomeron vertex corrections is a value of coefficient α_A from the Eq.22, see Fig.4. The LO DGLAP result gives $\alpha_A = 1$ for any value of Q^2 . As it seems from Fig.4, even at $Q^2 = 2.5 \text{ GeV}^2$ and $x \propto 10^{-3}$ the value of $\alpha_A \approx 0.8$ for the gold target. The obtained value is close to one and it is larger then the value of α_A obtained in [23], for example. The same parameterization as in Eq.22 we can write for the F_{2N} nuclei structure function, see Eq.25 and Eq.26. The calculations gives, that the F_{2N} structure function is less sensitive to the shadowing, i.e. the coefficient β_A is closer to unity then coefficient α_A in the same kinematical region.

The result of the anomalous dimension calculation for the case of the DIS on the proton, see Eq.28 and Fig.7, shows a significant dependence of the γ_P on the value of Q^2 . At large Q^2 and at small values of x , the $\gamma_P \rightarrow 1/2$, as it must be in the case of BFKL asymptotic results. For the smaller values of Q^2 the anomalous dimension is larger then half, that shows a corrections arise due the triple Pomeron vertex. The same calculations for the nuclei, see Fig.8, show a dependence of the value anomalous dimension of the nuclei on the atomic number A . This dependence especially underlined for the case of the small values of Q^2 , in contrary to the results of calculations in [23].

Another problem, considered in the paper, is a problem of the saturation momenta in the DIS on the proton and on the nuclei. First of all, initially we assumed a similar and factorized form for the saturation momenta of the proton and of the nuclei in the process of interest, see Eq.9 and Eq.13. The same factorized form was preserved in the final expressions for the saturation momenta of the proton and of the nuclei after the evolution over rapidity, see Eq.32 and Eq.34, that in some sense justify the calculations of [23, 25, 24] for example. Nevertheless, there is a principal difference between the calculations of the [23, 25, 24] and present one which must be underlined. In spite of the introducing the form of impact parameter dependence in the solution of evolution equation after evolution, as it was done in [23, 25, 24], the actual form of impact parameter dependence of the saturation momenta in the present framework is calculated through the rapidity evolution and, therefore the form of the saturation momenta with impact parameter dependence is different from the used in [23, 25, 24].

The performed calculation of the saturation scale shows, that we did not observe a suppression over atomic number in the expression for the saturation momenta, which was obtained in the similar calculations in different

papers, see for example [23, 37, 44, 45] and references therein, see Eq. (38) and plot in Fig.14. Still, we used a definition of saturation momenta different from the definition of [23], but our results are also different from the results of [37] where the similar definition was used. The first simple fact, which could explain this result, is that we obtained and used a different expression for the saturation momenta. Our expression contains two parts, one part of this expression is a constant and second part is a function which grows with rapidity. This future of the considered model may be explained by the local impact parameter dependence introduced in the calculations. From the Fig.9-Fig.13 we see, that in the large range of x the saturation momenta is almost a constant, the growth became at $x \propto 10^{-5}$ only. Considering the saturation momenta as the characteristic momenta of the scattering system which related with the averaged parton density of the system, we see, that until $x \propto 10^{-5}$ this density does not grow so fast. Therefore, the flatness of the saturation momenta as the function of x in broad small x region might be explained by the linear growth of target area in the impact parameter space accounted by the introduced impact parameter dependence. When a speed of increase of the area of the target is similar or larger than a speed of increase of the characteristic momenta then the saturation scale does not change so much. Only when the grow of the momenta is larger than the grow of the area of the target, only then we observe a increase of saturation momenta with the increasing of energy. We can conclude, therefore, that interplay between the linear growing of the area of the target in the impact parameter space and growing of the parton density "delays" growing of the saturation momenta. Only at asymptotically large energies, when the effect of the growth of the target area will be negligibly small, the expected suppression over the atomic number A perhaps could be observed .

Relating the proton and nuclei saturation momenta, see expression Eq. (38), we introduced a parameter $k_A(b)$ which is a parameter of the diluteness of the system, see [27]. As it was underlined in [27], see also references therein, this parameter is not so large for the case of real nucleus. Without discussing a new approaches introduced in [27] and a need of the additional rescattering corrections to the system amplitude, see for example [15], we can conclude nevertheless, that the relative smallness of this parameter shows on the smallness of the triple vertex (shadowing) corrections as well.

It is also interesting to compare obtained results with the other results on the saturation momenta. First of all, it is instructive to compare obtained form of the proton saturation momenta with the result of the GBW paper [17], see Fig.10. As it seems from the plot, the compared saturation scales have different functional form and also, as a consequence, different numerical values at different values of x . At relative large values of x the obtained in this paper saturation scale is larger then the GBW one, whereas at very small values of x the GBW is larger. The explanation of this result was done before, the difference arises mainly due the very different functional form of the functions. The expression Eq. (32) have a constant part which does depend on x , which arises because of the impact parameter dependence, and, therefore, the growth of the scale with the x decreases begins much later then in the GBW scale case. Therefore, it is difficult to compare our result with the different result based on the GBW scale parameterization and geometrical scaling application, see [44] for example. There the GBW saturation scale parameterization was used in order to extract the A^n dependence of the nuclei saturation momenta. Obtained in these calculations coefficient n is different from DGLAP $n = 1/3$ value obtained here, as it may be expected simply because of the different saturation scales parameterizations. Nevertheless, in the contrast to the results of [44] in the paper [43] the similar value of the coefficient $n = 1/3$ for the nuclei saturation scale was obtained after the light nuclei data excluding from the fitting procedure. Still, it must be underlined, that the compared models have a different calculation frameworks, that makes they comparison pretty difficult, see Appendix A for some remarks on this subject.

Obtained through the calculation expressions of the saturation momenta allow to investigate the scaling properties of the unintegrated gluon density function. In the given framework and in the considered kinematical

region we found that the scaling is only approximate future of the function as it seems from the Fig.11-Fig.12 and Fig.15-Fig.16. In general the unintegrated gluon density function depends on the two variables, scaling variable $\tau(b, x)$ and on the energy of the process (rapidity or value of x). Nevertheless, the scaling is precise when we fix the energy and consider different values of impact parameter. In this case, instead the different solutions at different impact parameters, the scaled solution arises and its depends only on the $\tau(b)$ variable.

Finally we would like to underline, that given calculations we consider as a first step in establishing of the framework for the investigation of more complex processes at very small values of x such as amplitude of proton-proton scattering at LNC energies or calculations of the amplitude of the exclusive Higgs boson production. The demonstration that in the framework of the interacting BFKL pomerons it is possible to describe a bulk of the DIS data on the proton and nuclei, leads us towards the application of the model in the calculations of these complex processes at the LHC collider energies.

Acknowledgments

S.B. especially grateful to Y.Shabelsky for the discussion on the subject of the paper. This work was done with the support of the Ministerio de Educacion y Ciencia of Spain under project FPA2005-01963 together with Xunta de Galicia (Conselleria de Educacion).

Appendix A:

In this appendix we would like to come back to some details concerning the DIS process on the proton from [4]. The main problem, which we faced in that calculations is a fail of the description of small $Q^2 < 1 \text{ GeV}^2$ DIS data for F_2 function, see details in [4]. If we will compare our approach with the saturation approach from [19, 29, 32], which describe all data of DIS on the proton, we immediately will see that we missed a correct description of gluon density function at small values of momenta, i.e. we do not reproduce the initial condition of DGLAP evolution equation for the DIS process. This result may be explained by the absence of the additional "net" diagrams in the BK approach. Indeed, when in the DIS process $Q^2 < Q_s^2$ then the use of only "fan" diagrams is acceptable. But when $Q^2 > Q_s^2$, i.e. when the size of projectile is large then the averaged size of partons in the proton, then we definitely miss additional contributions in the amplitude which represented by the "net" diagrams, see [39]. Taking into account that we obtain for the proton saturation momenta $Q_s^2 \approx 1 \text{ GeV}^2$ we see that indeed we have to face a problems when $Q^2 < 1 \text{ GeV}^2$.

Another hint to the solution of this problem is that during the calculations we obtain that the triple pomeron corrections are relatively small, see also Eq. (39) and [27]. Therefore, in spite of the long small x evolution we, as it seems, missed a correct initial DGLAP type condition in the region of small Q_s^2 which is crucially important in this kinematic region. So, as a resolution of the problem, it will be interesting to combine the DGLAP type initial conditions from the [19] with the BK evolution equation with local impact parameter dependence. This task we will leave for another publications.

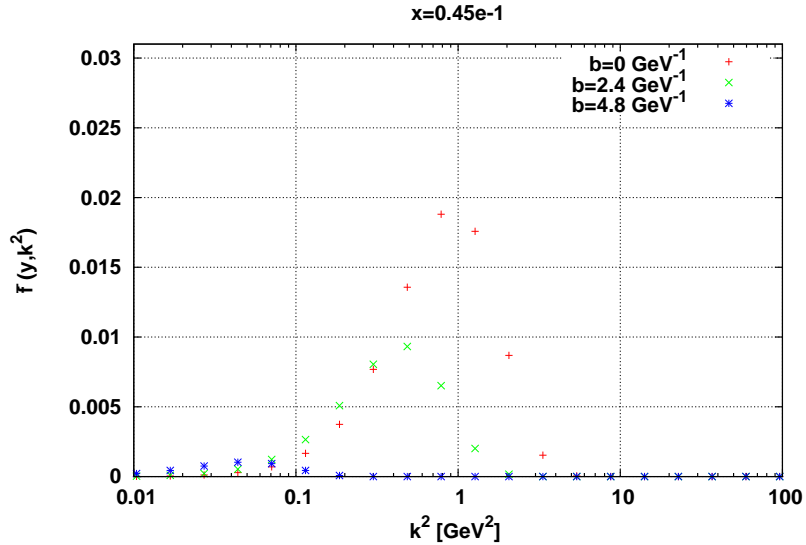


Figure 17: Initial profile of the unintegrated gluon density function $\tilde{f}(x, k^2, b)$ as a function of momenta k^2 at fixed values of x and different values of b for the case of DIS on the proton..

As a illustration of the difference between the present model and model of [19] we present here a plots of the unintegrated gluon density function Eq. (3) as a function of momenta at different values of x and impact parameter. This function has a dimension (as opposed to the dimensionless $\tilde{f}(x, k^2, b) / k^2$ function), therefore the numerical values of the function in the plots is not important and we also skip the dimension of the function on the plots. Nevertheless, it is interesting to trace a creation of the large k^2 tale of this function beginning from the initial condition, Fig.7, and through the small x evolution, Fig.7. Comparing this plots with the similar ones

from the [19] we see that our functions is absolutely different in the region of large k^2 , that may be explained as a result of the small x evolution. But there is a doubt that this tail explains a fail of the approach in the description of the F_2 function in the region of small Q^2 . This large k^2 tail affects on the exclusive processes mainly, whereas the inclusive ones are sensitive to the region of small k^2 which seems to be not so different from the presented in the [19].

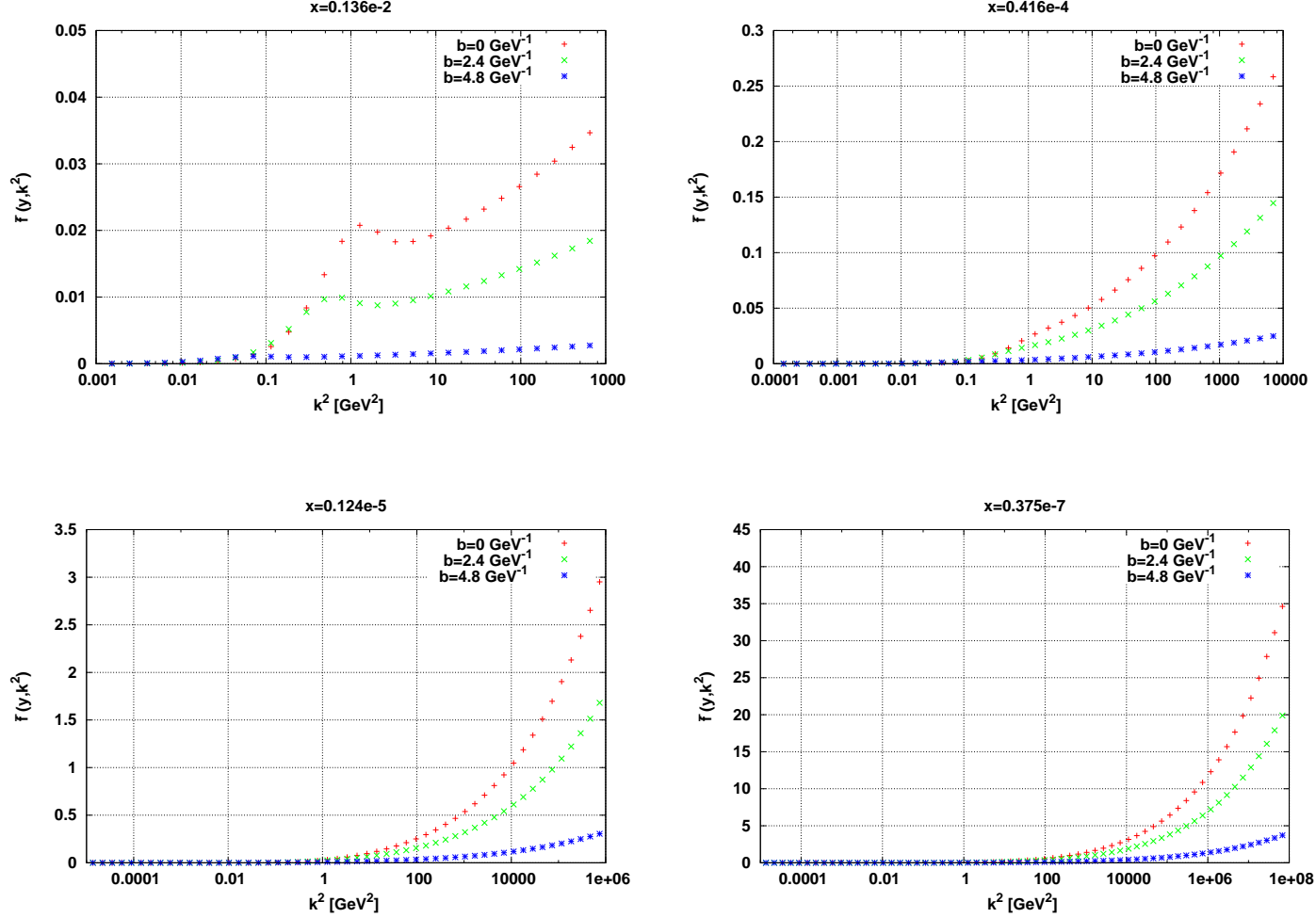


Figure 18: Unintegrated gluon density function $\tilde{f}(x, k^2, b)$ as a function of momenta k^2 at fixed values of x and different values of b for the case of DIS on the proton.

References

- [1] L. N. Lipatov, Phys. Rept. **286** 131(1997) ; Phys. Rept. **100** 1 (1983) .
- [2] I.I.Balitsky, Nucl. Phys. **B463** 99 (1996) .
- [3] Yu.V.Kovchegov, Phys. Rev. **D60** 034008 (1999) ; **D61** 074018 (2000) .
- [4] S. Bondarenko, Phys. Lett. B **665**, 72 (2008).
- [5] D. de Florian and R. Sassot, Phys. Rev. D **69**, 074028 (2004).
- [6] K. J. Eskola, V. J. Kolhinen and C. A. Salgado, Eur. Phys. J. C **9**, 61 (1999).
- [7] K. J. Eskola, H. Paukkunen and C. A. Salgado, JHEP **0807**, 102 (2008).
- [8] K. Tywoniuk, I. C. Arsene, L. Bravina, A. B. Kaidalov and E. Zabrodin, Eur. Phys. J. C **49**, 193 (2007).
- [9] M. A. Braun, Phys. Lett. B **483** 115 (2000).
- [10] M. A. Braun, Eur. Phys. J. C **33** 113 (2004) .
- [11] J. Bartels, S. Bondarenko, K. Kutak and L. Motyka, Phys. Rev. D **73**, 093004 (2006).
- [12] S. Bondarenko and L. Motyka, Phys. Rev. D **75**, 114015 (2007) .
- [13] E. Levin and A. Prygarin, arXiv:hep-ph/0701178.
- [14] S. Bondarenko, Nucl. Phys. A **792** 264 (2007).
- [15] S. Bondarenko and M. A. Braun, Nucl. Phys. A **799**, 151 (2008)
- [16] S. Bondarenko and A. Prygarin Nucl. Phys. A **800** 63 (2008).
- [17] K. J. Golec-Biernat and M. Wusthoff, Phys. Rev. D **59**, 014017 (1999)
- [18] K. J. Golec-Biernat and M. Wusthoff, Phys. Rev. D **60**, 114023 (1999).
- [19] J. Bartels, K. J. Golec-Biernat and H. Kowalski, Phys. Rev. D **66**, 014001 (2002).
- [20] A. H. Mueller, Nucl. Phys. B **335**, 115 (1990).
- [21] S. Munier, A. M. Stasto and A. H. Mueller, Nucl. Phys. B **603**, 427 (2001).
- [22] E. Gotsman, E. Levin, M. Lublinsky, U. Maor and K. Tuchin, Phys. Lett. B **492** (2000) 47
- [23] E. Levin and M. Lublinsky, Nucl. Phys. A **696**, 833 (2001)
- [24] E. Levin and M. Lublinsky, Nucl. Phys. A **712**, 95 (2002).
- [25] E. Gotsman, E. Levin, M. Lublinsky and U. Maor, Eur. Phys. J. C **27**, 411 (2003).
- [26] J. Bartels, E. Gotsman, E. Levin, M. Lublinsky and U. Maor, Phys. Rev. D **68**, 054008 (2003).
- [27] E. Levin and M. Lublinsky, Nucl. Phys. A **730** (2004) 191.
- [28] J. Kwiecinski, A. D. Martin and A. M. Stasto, arXiv:hep-ph/9706455.

- [29] H. Kowalski and D. Teaney, Phys. Rev. D **68**, 114005 (2003).
- [30] E. Iancu, K. Itakura and S. Munier, Phys. Lett. B **590**, 199 (2004).
- [31] J. L. Albacete, N. Armesto, J. G. Milhano, C. A. Salgado and U. A. Wiedemann, Phys. Rev. D **71** (2005) 014003.
- [32] H. Kowalski, L. Motyka and G. Watt, Phys. Rev. D **74**, 074016 (2006).
- [33] K. Kutak and J. Kwiecinski, Eur. Phys. J. C **29**, 521 (2003).
- [34] K. Kutak and A. M. Stasto, Eur. Phys. J. C **41**, 343 (2005).
- [35] K. Kutak, arXiv:hep-ph/0703068.
- [36] A. L. Ayala, M. B. Gay Ducati and E. M. Levin, Nucl. Phys. B **493**, 305 (1997).
- [37] N. Armesto and M. A. Braun, Eur. Phys. J. C **20**, 517 (2001)
- [38] J. Bartels and H. Kowalski, Eur. Phys. J. C **19**, 693 (2001).
- [39] S. Bondarenko, E. Gotsman, E. Levin and U. Maor, Nucl. Phys. A **683**, 649 (2001).
- [40] C. W. De Jager, H. De Vries and C. De Vries, Atom. Data Nucl. Data Tabl. **36** (1987) 495.
- [41] P. Amaudruz *et al.* [New Muon Collaboration], Z. Phys. C **51** (1991) 387.
- [42] P. Amaudruz *et al.* [New Muon Collaboration], Nucl. Phys. B **441** (1995) 3.
- [43] A. Freund, K. Rummukainen, H. Weigert and A. Schafer, Phys. Rev. Lett. **90** (2003) 222002.
- [44] N. Armesto, C. A. Salgado and U. A. Wiedemann, Phys. Rev. Lett. **94** (2005) 022002.
- [45] H. Kowalski, T. Lappi and R. Venugopalan, Phys. Rev. Lett. **100** (2008) 022303.